

Article

Identification of the Sedimentary Sources and Origin of Uranium for Zhiluo Formation of the Tarangaole U Deposit, Northeastern Ordos Basin

Guang-Yao Li ^{1,2,3,*}, Chun-Ji Xue ¹, Qiang Zhu ^{2,3,*}, Jian-Wen Yang ⁴ and Xiao-Bo Zhao ¹ 

¹ School of Earth Sciences and Resources, China University of Geosciences, Beijing 100083, China; chunji.xue@cugb.edu.cn (C.-J.X.); xiaobozhao@cugb.edu.cn (X.-B.Z.)

² Tianjin Center, China Geological Survey (North China Center for Geoscience Innovation), Tianjin 300170, China

³ Key Laboratory of Uranium Geology of China Geological Survey, Tianjin 300170, China

⁴ School of the Environment, University of Windsor, Windsor, ON N9B 3P4, Canada; jianweny@uwindsor.ca

* Correspondence: lgy@email.cugb.edu.cn (G.-Y.L.); zqiang@mail.cgs.gov.cn (Q.Z.)

Abstract: The large-sized Tarangaole uranium deposit and its neighboring Daying and Nalinggou deposits, located in the northeastern margin of the Ordos Basin, constitutes a major uranium resource base in northern China. In order to further clarify the sedimentary material source, uranium source and regional sediment–tectonic setting of the uranium-fed clastic rocks (i.e., Zhiluo Formation(J_{2z})) in the district, this paper carried out whole-rock geochemistry, heavy minerals composition and in situ U-Pb dating of detrital zircons for sandstones from the lower section of the Zhiluo Formation. The results have shown that the average chemical differentiation index (CIA) for the host rocks is 73.16 and the chemical weathering degree is moderate. Heavy minerals are mainly composed of ilmenite, garnet, chlorpyrite, zircon, pyrite, apatite, hematite, etc. The U-Pb dating of detrital zircon generally indicates three age peaks, i.e., 260~Ma, 1850~Ma and 2450~Ma, respectively. In conclusion, the source rocks may have been formed at active continental margins, e.g., in a continental margin arc environment. The sedimentary materials mainly come from khondalite series, TTGs, granulite, and mafic-ultramafic intrusive rocks distributed among the Daqing–Ula Mountains and adjacent areas, etc. The Late Paleozoic U-rich intermediate and acidic magmatic rocks spreading over the eastern part of the Ula–Daqing and Wolf mountains have provided the main uranium sources for the formation of major U deposits in the northern Ordos Basin.

Keywords: sandstone-type uranium deposit; sedimentary source; heavy minerals; detrital zircon dating; tarangaole; Ordos Basin



Citation: Li, G.-Y.; Xue, C.-J.; Zhu, Q.; Yang, J.-W.; Zhao, X.-B. Identification of the Sedimentary Sources and Origin of Uranium for Zhiluo Formation of the Tarangaole U Deposit, Northeastern Ordos Basin. *Minerals* **2024**, *14*, 429. <https://doi.org/10.3390/min14040429>

Academic Editor: Davide Lenaz

Received: 5 February 2024

Revised: 18 April 2024

Accepted: 18 April 2024

Published: 20 April 2024



Copyright: © 2024 by the authors. Licensee MDPI, Basel, Switzerland. This article is an open access article distributed under the terms and conditions of the Creative Commons Attribution (CC BY) license (<https://creativecommons.org/licenses/by/4.0/>).

1. Introduction

The Ordos Basin is an important energy basin in northern China, in coexistence with coal, oil, gas, uranium and other mineral resources [1]. The northeastern margin of the Ordos Basin has been a research hotspot for sandstone-type uranium deposits. The Tarangaole uranium deposit, located between the Daying super-large and the Nalinggou large-sized uranium deposits, is a newly discovered large-sized uranium deposit in this district. The Daying–Tarangaole–Nalinggou uranium deposits constitute a large uranium resource base in northern China [2]. The uranium-bearing strata of the three deposits are the Middle Jurassic Zhiluo Formation. The analysis of the sedimentary material sources of the Zhiluo Formation can provide an important basis for the study of the coupling mineralization process, uranium sources and mineralization mechanism in the northeast margin of the Ordos Basin. Previously, whole-rock geochemistry, mineralogy, hydrothermal alteration and detrital zircon U-Pb dating have been carried out for uranium deposits such as the Daying and Nalinggou deposits [3–9]. These studies have presented some understanding of their

geochemical characteristics, fluid alteration characteristics, mineralization mechanisms and metallogenetic patterns. As a newly discovered deposit, the source of mineralization and its regional sedimentary–tectonic setting of the Tarangaole deposit are poorly constrained. This has limited our understanding for the Zhiluo Formation of sedimentary sources, evolution and further uranium prediction and evaluation in the uranium resource base.

In this paper, based on a systematic investigation on coalfield and uranium deposits boreholes, some basic work, such as the geochemistry, detrital zircon U-Pb geochronology and heavy minerals composition for the sandstones in the lower section of the Zhiluo Formation, was carried out in the Tarangaole area. Furthermore, in combination with regional geological background and isotopic chronologic data from the regional Precambrian metamorphic rocks and intrusive rocks, the origination, evolution and tectonic setting for the uranium-containing Zhiluo Formation are discussed. The relevant results provide key insights for the further exploration of the sandstone-type uranium deposit in the northeastern Ordos Basin mining district.

2. Geological Setting

The research area is located at the Tarangaole, north-central part of the Yimeng Uplift, Ordos Basin (Figure 1), and is situated to the south of the Hetao graben and Yinshan orogenic belt. Within this area, the well-known Daying uranium deposit lies in the west, the Nalinggou uranium deposit lies in the east and the three deposits are located approximately 10–15 km from each other. Regionally, the Carboniferous to Quaternary successively were deposited on Archean and Proterozoic basement rocks and the overall strata show a monoclinic structure gently dipping towards the south-west direction. The Poerjianghaizi deep fault is located near the study area and cuts deeply into the basement. The sandstone-type uranium deposits are hosted in the Middle Jurassic Zhiluo Formation (J_{2z}) [10]. This formation unconformably overlies the coal-bearing strata of the Yan'an Formation (J_{1-2y}) and is in conformable contact with the overlying Anding Formation (J_{2a}). Due to the uneven erosion of the Anding Formation, the Lower Cretaceous conglomerates unconformably cover the top of the Zhiluo Formation in some areas [11]. Two capital ancient river channels spread from north to south in the Tarangaole area [8], evolving into multiple branches to the south (Figure 1). The width of the channel is 5~10 km, the thickness can reach up to 260 m and the arenite content can reach up to 85%.

The thickness of the Zhiluo Formation in the study area is 130~400 m and the bottom boundary is buried at a depth of 300~800 m (Figure 2a,b). The Zhiluo Formation can be divided into upper and lower sections according to their lithology (Figure 2c,d). The lower section (J_{2z}^1) is dominated by gray and gray-green medium-coarse sandstone, with gravel at the bottom, and the proportion of sandstone is generally more than 75%, which presents typical sedimentation of braided fluvial facies [12]. In the upper section (J_{2z}^2), the argillaceous interlayer increases significantly and the grain size becomes finer. The upper stratum is mainly composed by gray-green medium-fine-grained sandstone, brown-red mudstone and siltstone. The uranium ore bodies, which are distributed in the transition part of the gray-green alteration zone and the gray reduction zone of the Zhiluo Formation (J_{2z}^1), appear in the form of board and rolls on the profile. The lower section of the Zhiluo Formation presents loose, coarse-grained, mainly gray and gray-white conglomerate sandstone and coarse sandstone in the northern part of the study area; it gradually changes to gray and gray-green medium sandstone and fine sandstone. The main mineral components of the sandstone of the Zhiluo Formation are: quartz, feldspar and granite detritus, etc. Mineral sorting is medium-fine and the rounding is general-medium-sized (Figure 2e,f). The thickness of gray-green uranium-bearing sandstone can generally reach up to 50~100 m (Figure 2g).

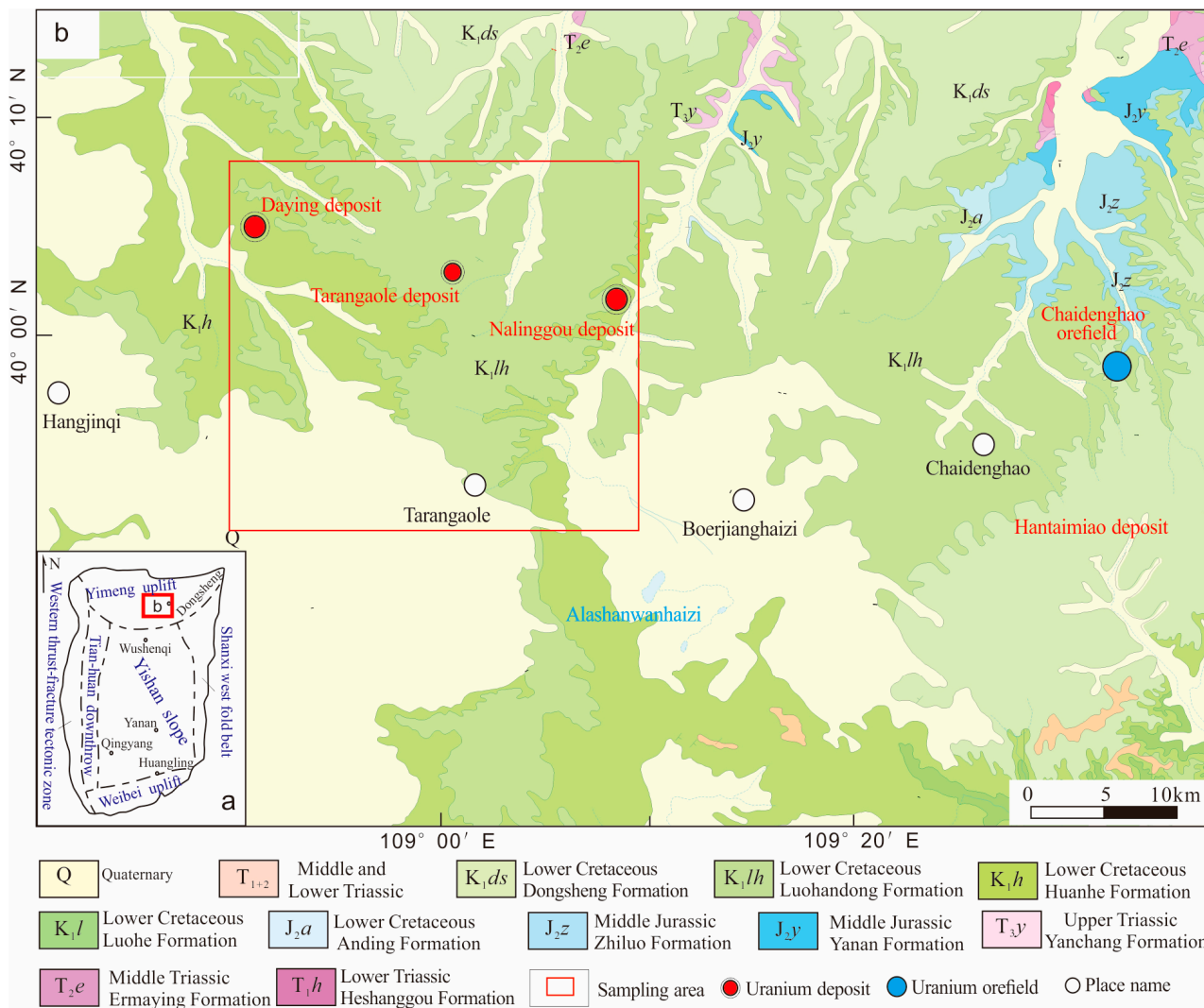


Figure 1. Schematic tectonic map of the Ordos Basin (a) and regional geological map of research area (b) (modified from [3]).

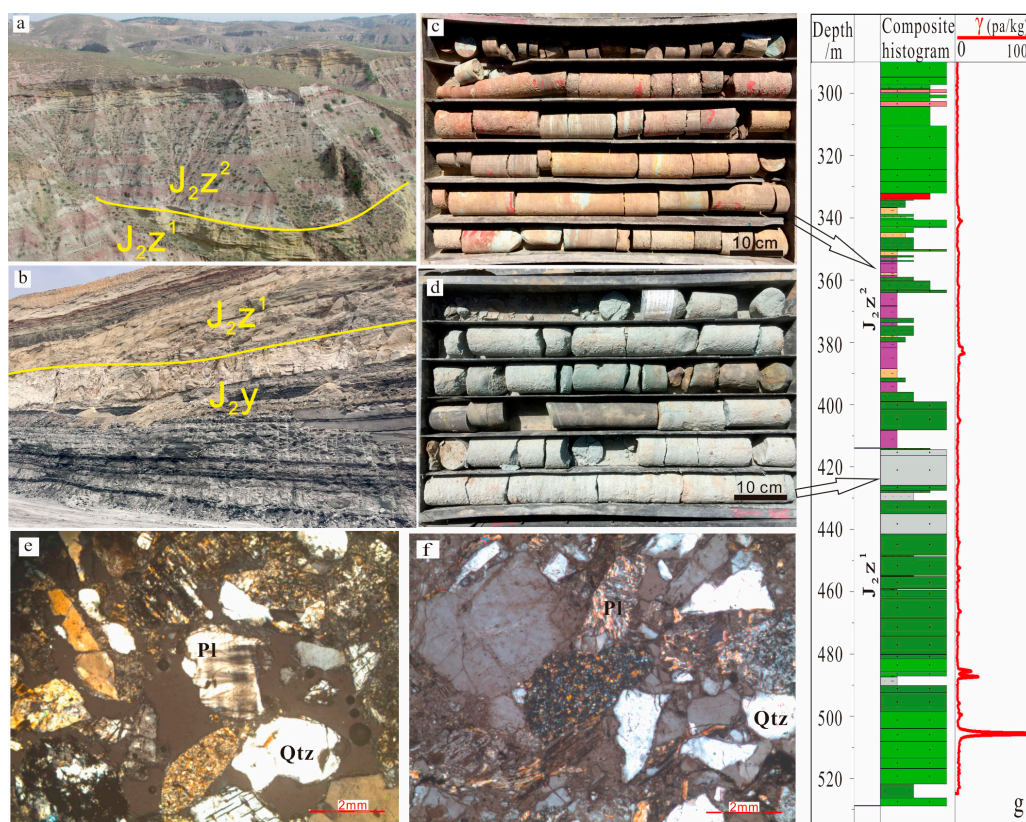


Figure 2. Field outcrops, drill core photographs and stratigraphic histogram of the Tarangaoe uranium deposit. (a) Outcrops of the upper and lower subsection of the lower section from the Zhiluo Formation; (b) Outcrops of the Zhiluo and Yan'an formations; (c) Drilled cores from the upper section of the Zhiluo Formation; (d) Drilled cores from the lower section of the Zhiluo Formation; (e,f) Microscopic feature of the Zhiluo Formation greywacke; (g) Schematic stratigraphic column of the Zhiluo Formation. Qtz = quartz, Pl = plagioclase.

3. Sampling and Analytical Methods

3.1. Sampling

Clastic rock samples from the boreholes were collected from the Zhiluo Formation in the Tarangaoe and Nalinggou deposit area. All samples were processed at the Laboratory of Beijing Institute of Geology, Nuclear Industry, and the Laboratory of Tianjin Center, China Geological Survey.

3.2. Analytical Methods

3.2.1. Petrogeochemistry

Seven sandstone samples were used for the petrogeochemistry analysis. The major elements analysis was carried out by melting X-ray fluorescence spectroscopy (XRF) method and the Inductively coupled plasma-Mass Spectrometry (ICP-MS) method was used for trace and rare earth elements analysis at the Laboratory of Beijing Institute of Geology, Nuclear Industry. The analysis accuracy for major and trace elements are better than 5%.

3.2.2. Heavy Mineral Analysis

Heavy minerals analysis was performed on 19 medium-sized to coarse-grained sandstone samples and the sampling location is shown in Figure 1. Sixteen samples were taken from the borehole cores in the Tarangaoe area, whereas 3 samples were collected from outcrop profile in the Gaotouyao area, covering the entire Zhiluo Formation distribution in the northern basin. Each sample (mainly medium-coarse-grained sandstone) weighed 1~3 kg. The samples were processed as following: the weathered parts of the sample were

removed, crushed, acidified and then selected as 63~250 μm mixed particle level fragments. Minerals were separated by the heavy liquid (CHBr_3) method, then about 20 mg heavy minerals were identified under the binocular.

3.2.3. Zircon U-Pb Dating

The detrital zircons from fine-grained sandstone samples were collected for in situ LA-ICP-MS U-Pb dating. The separation of zircon grains and production of sample targets were undertaken by Langfang Chengxin Geological Service Co., Ltd. (Hebei, China). Zircon U-Pb isotope dating was conducted at the Laboratory of the Tianjin Center, China Geological Survey, using a Neptune (LA-MC-ICPMS) manufactured by Thermo Fisher Scientific, Waltham, MA, USA, referring to [13] and [14] for detailed procedures. The age data were processed by the ICPMS Data Cal program [15] and the calculation of zircon weighted average age and drawing of concordia diagrams were finished by Isoplot [16].

4. Results

4.1. Petrogeochemistry

The results of the major element analysis are shown in Table 1. The SiO_2 content of the Zhiluo Formation sandstone in the Tarangaole area is relatively low, averaging at 64.14%. The content of Al_2O_3 is higher, with an average content of 15.98%. In addition, the average chemical differentiation index (CIA) of the Zhiluo Formation sandstone is 73.16, indicating that the chemical weathering degree is moderate at the source area.

Table 1. Major elements (%) of analytical data of the Zhiluo Formation sandstone in study area.

Sample	UZK2-31	UZK13-43	UZK13-38	UZK13-40	UZK13-58	ZKC2016-1-40	UZK38-23
SiO_2	65.98	66.54	64.55	63.23	62.10	64.87	61.68
Al_2O_3	16.20	15.54	16.27	16.50	14.96	14.82	17.57
Fe_2O_3	2.26	2.90	3.38	4.22	3.86	4.94	2.93
FeO	1.70	1.21	1.73	1.50	4.50	0.64	2.89
T Fe_2O_3	4.15	4.24	5.30	5.89	8.86	5.65	6.14
CaO	1.02	1.30	1.09	1.14	1.12	1.80	1.19
MgO	2.24	2.02	2.19	2.44	3.05	2.36	2.67
K_2O	3.28	3.13	3.21	3.05	3.09	2.84	2.88
Na_2O	1.58	1.86	1.59	1.76	1.12	1.32	1.61
TiO_2	0.77	0.79	0.83	0.87	0.75	0.77	0.86
P_2O_5	0.16	0.03	0.14	0.19	0.20	0.19	0.10
MnO	0.05	0.06	0.06	0.06	0.08	0.05	0.07
LOI	4.59	4.49	4.77	4.87	4.68	5.34	5.24
Totals	99.83	99.87	99.81	99.83	99.51	99.94	99.69
CIA	73.37	71.19	73.42	73.50	73.73	71.32	75.57

CIA indicates the chemical differentiation index of sedimentary rock sources; CIA = $[\text{Al}_2\text{O}_3 / (\text{Al}_2\text{O}_3 + \text{CaO} + \text{Na}_2\text{O} + \text{K}_2\text{O})] \times 100$ and the content of each oxide in the formula is molar mass.

The analysis results of trace and rare earth elements (REE) are shown in Table 2. The contents of compatible elements such as Co, Ni, Cr and V are similar to average levels of the continental crust [17], showing a moderately acidic tendency. In the MORB-normalized trace element spider diagram (Figure 3a), these rocks are relatively enriched in large-ion lipophile elements (LILEs) such as K, Rb and Ba, and depleted in high-field-strength elements (HFSEs) (e.g., Ti and Ta) and inactive elements such as P, as well as Sr, Ni and Y. The total amount of REEs for the Zhiluo sandstones varies significantly (192.42~292.32 ppm) with an average of 241.82 ppm. The $\Sigma\text{LREE}/\Sigma\text{HREE}$ ratios fall into 4.46 to 5.27, with an average ratio of 4.65. The $(\text{La}/\text{Yb})_{\text{N}}$ is varying from 10.79 to 13.03 with an average ratio of 11.80. According to the distribution mode of REEs (Figure 3b), most of the samples have no obvious Ce anomalies. The chondrite-normalized patterns show that the light REE tends to be enriched, whereas heavy REEs are flat, with δEu 0.66~0.77 (the average 0.73). The weak Eu negative anomaly and the REE mode is similar to that of the upper crust [18].

Table 2. Trace elements (weight-ppm) and rare earth elements (weight-ppm) analytical data of the Zhiluo Formation sandstone.

Sample	UZK2-31	UZK13-43	UZK13-38	UZK13-40	UZK13-58	ZKC2016-1-40	UZK38-23
Cu	16.5	30.6	36.8	31.2	34.8	22	36
Pb	13.2	18.4	16.1	19.6	14.4	18.4	26.1
Zn	77.4	82.5	79.8	89	88.1	60.4	91.8
Cr	88.6	121.	111	103	79.5	215	98
Ni	37.4	37	35.6	47.6	30.1	35.8	40.4
Co	19.4	19.9	18.6	23	18	18	20.6
Cd	0.03	0.03	0.03	0.04	0.04	0.08	0.11
Li	42.2	25.7	31.5	33.6	35.6	23	57.6
Rb	118	118	119	119	116	61.3	105
Cs	5.06	5.73	5.63	6.3	5.34	3.24	7.23
W	0.8	0.96	0.81	0.94	0.9	0.98	1.41
Mo	0.32	1.89	0.47	1.62	0.41	8.25	0.58
Sb	0.16	0.15	0.21	0.2	0.16	0.17	0.26
Bi	0.13	0.1	0.22	0.28	0.12	0.12	0.46
Sr	321	361	364	366	322	319	403
Ba	929	814	840	787	786	820	720
V	84.6	93.	99.5	118	127	102	120
Sc	13.4	12.2	11	14.9	13.2	13.8	15.6
Be	1.83	1.64	2	2.08	2.69	1.54	2.9
Ga	20.6	21.3	21.5	23.2	24.7	19.2	24.1
U	2.19	5.2	5.18	5.51	5.19	1.74	3.41
Th	9.64	9.54	9.63	10.8	12.9	8.41	14.8
La	36.8	41.2	42.5	48.4	52.4	40.6	56
Ce	73.6	87	98.4	108	101	88.9	116
Pr	8.06	8.97	9.52	10.7	10.7	9.17	11.6
Nd	31.4	35.1	37.8	42.7	41.3	36.6	45.8
Sm	5.89	6.48	6.85	8.12	7.54	6.86	8.64
Eu	1.41	1.5	1.6	1.86	1.86	1.66	1.84
Gd	5.37	5.99	6.21	7.72	7.09	6.23	8.04
Tb	0.75	0.83	0.83	1.05	0.99	0.87	1.13
Dy	4.13	4.61	4.41	5.74	5.54	4.72	6.24
Ho	0.74	0.84	0.78	1.01	1.02	0.86	1.11
Er	2.04	2.34	2.13	2.7	2.8	2.4	3.07
Tm	0.33	0.38	0.34	0.42	0.45	0.38	0.5
Yb	2.26	2.61	2.34	2.84	3.1	2.7	3.51
Lu	0.34	0.41	0.35	0.44	0.49	0.42	0.54
Y	19.3	22.4	19.9	25.2	26.5	21.3	28.3
ΣREE	192.42	220.66	233.96	266.9	262.78	223.67	292.32
LREE	157.16	180.25	196.67	219.78	214.8	183.79	239.88
HREE	35.26	40.41	37.29	47.12	47.98	39.88	52.44
LREE/HREE	4.46	4.46	5.27	4.66	4.48	4.61	4.57
δEu	0.75	0.72	0.74	0.71	0.77	0.76	0.66
(La/Yb) _N	11.68	11.32	13.03	12.22	12.12	10.79	11.44
(Gd/Yb) _N	1.97	1.9	2.2	2.25	1.89	1.91	1.89

$\delta\text{Eu} = 2\text{Eu}_N / (\text{Sm}_N + \text{Gd}_N)$; N after [20].

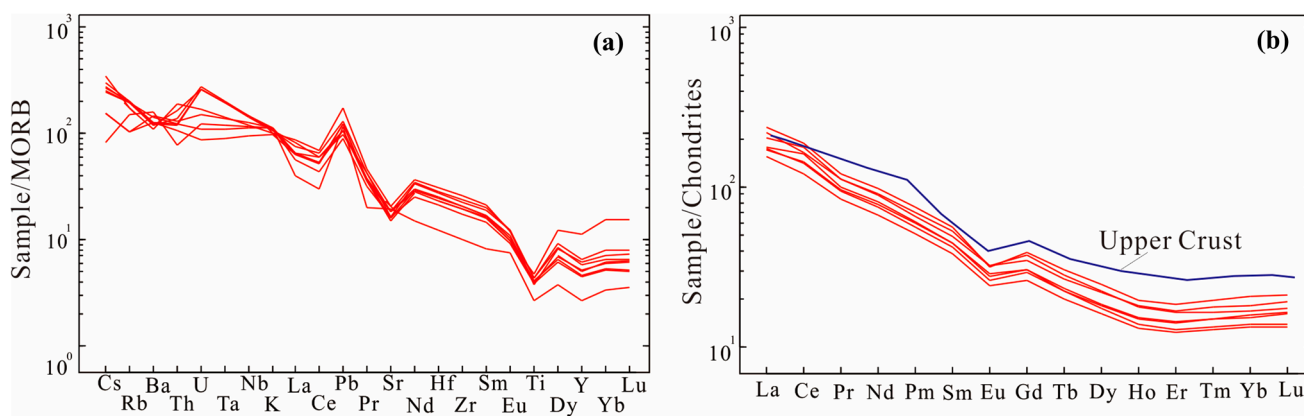


Figure 3. MORB-normalized trace element spider diagram (a) (after [19]) and chondrite-normalized REE pattern (b) (after [20]) of sandstones from the Zhiluo Formation in study area.

4.2. Heavy Mineral Analysis

The statistical results of heavy minerals in the study area are shown in Figure 4. The main heavy minerals in the Zhiluo Formation sandstones are ilmenite, zoisite and garnet (>40%), followed by zircon, pyrite, apatite, hematite, etc., (within 10%). Especially noteworthy is that pyrite minerals are concentrated in the middle of the study area, spreading in a north–south band, whereas hematite minerals are relatively concentrated in the outer area (Figure 4).

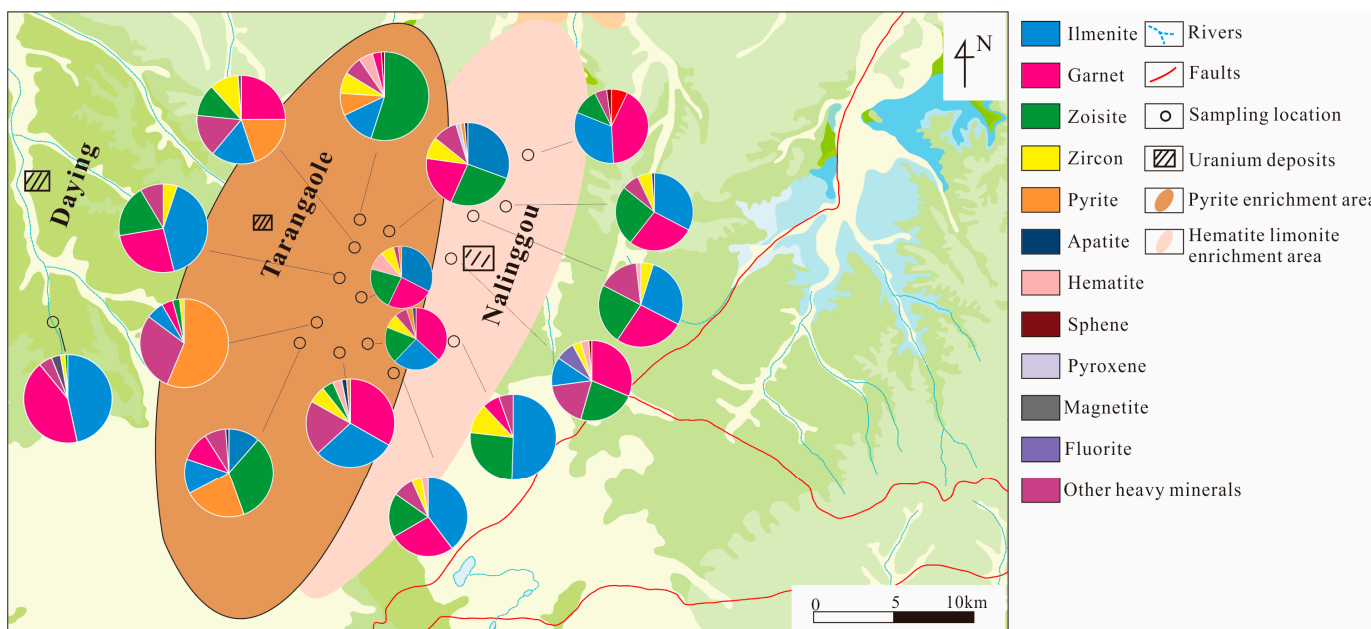


Figure 4. Comparison of heavy mineral contents within sandstones from Zhiluo Formation in the Tarangaole uranium deposit, Ordos Basin.

4.3. Zircon U-Pb Geochronology

According to the cathodoluminescence (CL) images (Figure 5), it can be seen that the zircon grains are medium in size (60~120 μm), the crystals are idiomorphic and hypidiomorphic and the growth ring and oscillatory zoning are obvious. Among them, the Paleozoic grains are mostly angular, indicating a magmatic source. In contrast, the older zircons are mostly round and some of them have ancient cores, indicating that they may have experienced long-distance transport abrasion and later metamorphic recrystallization [21].

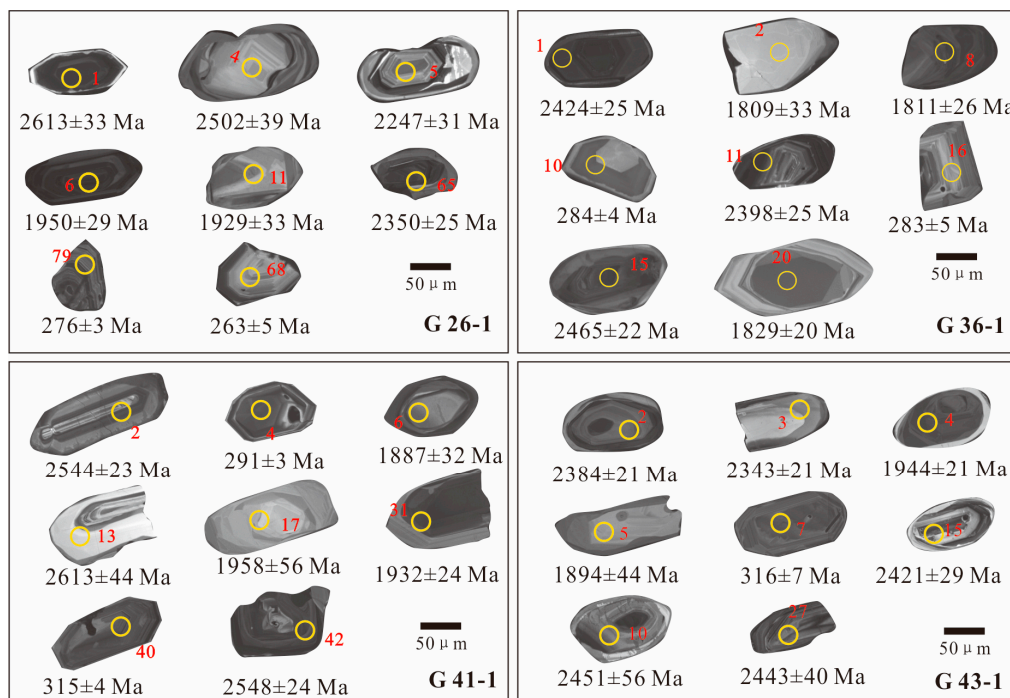


Figure 5. Carhodoluminescence (CL) images of typical detrital zircon from sandstone samples (G26-1, G36-1, G41-1 and G43-1) of the Zhiluo Formation.

Based on the geochronological results (Tables 3–6), the $^{206}\text{Pb}/^{238}\text{U}$ surface age was adopted for the individual zircon (<1000 Ma); the $^{207}\text{Pb}/^{206}\text{Pb}$ surface age was also adopted (>1000 Ma) [22] (Figure 5). Most of the data points fall on or near a concordia line, after removing the concordia degree < 95%. Only a few points deviated slightly from the concordia line, reflecting the little loss of Pb or U.

Eighty zircon grains from Sample G26-1 were tested (Table 3), of which four zircon grains had a concordia degree of less than 95%, without participating in the age statistics. The concordia age of 76 zircon grains is mainly divided into three groups: group 1, with an age of 240~277 Ma and a main peak of ~262 Ma; group 2, with an age of 1817~1989 Ma and a main peak of ~1956 Ma; and group 3, with an age of 2247~2668 Ma and peaks of 2335 Ma and 2512 Ma (Figure 6a,b).

Ninety-five zircon grains from Sample G36-1 were tested (Table 4), of which one zircon grain presented a concordia degree of less than 95%, without participating in the age statistics. The concordia age of 94 zircon grains can be divided into three groups: group 1, with an age of 260~323 Ma and a peak of ~280 Ma; group 2, with an age of 1643~2035 Ma and peaks of ~1828 Ma and ~2000 Ma; and group 3, with an age of 2172~2736 Ma and a peak of ~2450 Ma (Figure 6c,d).

Eighty-eight zircon grains from Sample G41-1 were tested (Table 5), of which three zircon grains present a concordia degree of less than 95%, without participating in the age statistics. The concordia age of 85 zircon grains could be divided into three groups: group 1, aged between 264~335 Ma with a main peak of ~315 Ma; group 2, with an age of 1767~2200 Ma and peak ages of ~1850 Ma, 1960 Ma and ~2020 Ma; and group 3, with an age of 2256~2785 Ma and a main peak of ~2531 Ma (Figure 6e,f).

Eighty zircon grains from Sample G43-1 were tested (Table 6), of which eight zircon grains presented a concordia degree of less than 95%, without participating in the age statistics. The concordia age of 72 zircon grains can be divided into three groups: group 1, aged between 275~326 Ma with a peak of ~265 Ma; group 2, with an age of 1700~2200 Ma and a main peak of ~1829 Ma and ~1997 Ma; and group 3, with an age of 2200~3000 Ma and a peak of ~2418 Ma (Figure 6g,h).

Table 3. U-Pb isotope test results of detrital zircon from the Zhiluo Formation sandstone (G26-1) in study area.

Point No.	Content ($\times 10^{-6}$)			Isotope Ratio						Age (Ma)						Concordia
	Pb	Th	U	$^{207}\text{Pb}/^{206}\text{Pb}$	1σ	$^{207}\text{Pb}/^{238}\text{U}$	1σ	$^{206}\text{Pb}/^{238}\text{U}$	1σ	$^{207}\text{Pb}/^{206}\text{Pb}$	1σ	$^{207}\text{Pb}/^{235}\text{U}$	1σ	$^{206}\text{Pb}/^{238}\text{U}$	1σ	Concordia
01	177	52	262	0.1756	0.0035	11.9518	0.2516	0.4925	0.0047	2613	33	2601	20	2581	20	99%
02	21	44	43	0.1121	0.0030	4.9818	0.1413	0.3226	0.0041	1835	49	1816	24	1803	20	99%
03	192	132	218	0.2153	0.0036	17.3132	0.3987	0.5806	0.0091	2946	27	2952	22	2951	37	99%
04	22	37	29	0.1644	0.0038	10.6738	0.2775	0.4705	0.0063	2502	39	2495	24	2486	28	99%
05	75	85	125	0.1416	0.0025	8.3593	0.1814	0.4269	0.0058	2247	31	2271	20	2292	26	99%
06	164	105	359	0.1196	0.0019	5.8697	0.1103	0.3550	0.0037	1950	29	1957	16	1958	18	99%
07	375	216	1105	0.1170	0.0020	4.2323	0.0909	0.2616	0.0036	1911	30	1680	18	1498	19	88%
08	25	69	48	0.1110	0.0026	4.9106	0.1250	0.3203	0.0040	1817	42	1804	22	1791	20	99%
09	117	259	364	0.1606	0.0027	4.9063	0.0993	0.2211	0.0031	2462	27	1803	17	1288	17	66%
10	158	230	242	0.1503	0.0023	9.0279	0.1472	0.4345	0.0035	2350	26	2341	15	2326	16	99%
11	18	33	36	0.1182	0.0025	5.7714	0.1306	0.3545	0.0043	1929	33	1942	20	1956	20	99%
12	145	208	194	0.1675	0.0031	11.0229	0.1961	0.4760	0.0055	2533	31	2525	17	2510	24	99%
13	112	138	162	0.1631	0.0026	10.7611	0.1943	0.4766	0.0048	2489	28	2503	17	2512	21	99%
14	34	79	41	0.1642	0.0032	10.8831	0.2434	0.4786	0.0059	2500	33	2513	21	2521	26	99%
15	27	30	53	0.1267	0.0026	6.6853	0.1567	0.3821	0.0057	2054	36	2071	21	2086	26	99%
16	40	66	51	0.1671	0.0035	11.2854	0.2820	0.4862	0.0069	2529	35	2547	23	2554	30	99%
17	235	305	359	0.1628	0.0028	10.4647	0.1999	0.4640	0.0049	2487	28	2477	18	2457	22	99%
18	210	227	350	0.1475	0.0023	8.9483	0.1632	0.4380	0.0048	2318	28	2333	17	2342	21	99%
19	6	113	106	0.0514	0.0023	0.2863	0.0130	0.0407	0.0007	257	106	256	10	257	4	99%
20	51	48	100	0.1302	0.0022	7.1021	0.1404	0.3938	0.0045	2102	30	2124	18	2140	21	99%
21	525	460	926	0.1419	0.0023	8.2255	0.1389	0.4193	0.0059	2250	23	2256	15	2257	27	99%
22	119	167	202	0.1470	0.0022	8.7093	0.1586	0.4278	0.0050	2322	25	2308	17	2296	22	99%
23	47	49	63	0.1817	0.0035	12.7379	0.2575	0.5074	0.0053	2668	32	2660	19	2645	23	99%
24	204	220	334	0.1470	0.0023	8.7236	0.1581	0.4288	0.0047	2322	27	2310	17	2300	21	99%
25	18	35	49	0.0957	0.0026	3.6207	0.0945	0.2743	0.0030	1543	46	1554	21	1563	15	99%
26	213	245	349	0.1495	0.0022	9.0416	0.1757	0.4370	0.0064	2340	25	2342	18	2337	29	99%
27	200	180	315	0.1601	0.0022	10.4757	0.1943	0.4736	0.0078	2457	23	2478	17	2500	34	99%
28	14	225	227	0.0516	0.0032	0.3126	0.0192	0.0439	0.0008	333	143	276	15	277	5	99%
29	20	242	371	0.0508	0.0012	0.2902	0.0071	0.0413	0.0004	232	56	259	6	261	3	99%
30	8	71	119	0.0524	0.0051	0.3837	0.0394	0.0526	0.0013	306	229	330	29	330	8	99%
31	27	40	56	0.1159	0.0021	5.5991	0.1152	0.3495	0.0045	1894	33	1916	18	1932	22	99%
32	516	854	1076	0.1505	0.0024	6.7355	0.1191	0.3226	0.0032	2352	32	2077	16	1802	16	85%
33	146	112	301	0.1286	0.0019	6.7466	0.1219	0.3785	0.0049	2080	26	2079	16	2069	23	99%
34	157	224	248	0.1523	0.0021	9.2912	0.1425	0.4405	0.0043	2371	22	2367	14	2353	19	99%
35	170	143	249	0.1715	0.0022	11.6570	0.2174	0.4899	0.0069	2572	22	2577	18	2570	30	99%
36	4	34	55	0.0561	0.0073	0.4152	0.0439	0.0557	0.0021	457	262	353	31	349	13	99%
37	422	428	647	0.1598	0.0023	10.1828	0.1655	0.4603	0.0062	2454	24	2452	15	2441	27	99%
38	208	215	365	0.1477	0.0020	8.7802	0.1432	0.4294	0.0048	2319	22	2315	15	2303	22	99%
39	45	74	67	0.1557	0.0027	9.7907	0.2446	0.4538	0.0081	2409	25	2415	23	2412	36	99%
40	87	78	139	0.1598	0.0026	10.3088	0.2010	0.4665	0.0062	2454	28	2463	18	2468	27	99%
41	89	102	130	0.1646	0.0024	11.0402	0.1873	0.4847	0.0052	2503	24	2527	16	2548	23	99%

Table 3. Cont.

Point No.	Content ($\times 10^{-6}$)				Isotope Ratio				Age (Ma)				Concordia			
	Pb	Th	U	$^{207}\text{Pb}/^{206}\text{Pb}$	1 σ	$^{207}\text{Pb}/^{235}\text{U}$	1 σ	$^{206}\text{Pb}/^{238}\text{U}$	1 σ	$^{207}\text{Pb}/^{206}\text{Pb}$	1 σ	$^{207}\text{Pb}/^{235}\text{U}$	1 σ	$^{206}\text{Pb}/^{238}\text{U}$	1 σ	
42	23	69	43	0.1143	0.0024	5.2691	0.1231	0.3333	0.0038	1869	39	1864	20	1855	18	99%
43	243	85	434	0.1497	0.0035	8.9756	0.2301	0.4332	0.0114	2342	41	2336	23	2320	51	99%
44	118	66	271	0.1193	0.0018	5.8959	0.1149	0.3572	0.0050	1946	27	1961	17	1969	24	99%
45	21	62	48	0.1085	0.0022	4.6236	0.0968	0.3103	0.0040	1776	37	1754	18	1742	20	99%
46	62	75	93	0.1626	0.0025	10.7826	0.2194	0.4788	0.0070	2483	26	2505	19	2522	30	99%
47	81	93	128	0.1592	0.0024	10.0285	0.1773	0.4553	0.0050	2447	26	2437	16	2419	22	99%
48	240	367	322	0.1654	0.0025	10.7398	0.1867	0.4688	0.0050	2522	26	2501	16	2478	22	99%
49	92	110	210	0.1151	0.0019	5.3521	0.1061	0.3350	0.0042	1883	36	1877	17	1863	20	99%
50	46	47	103	0.1175	0.0022	5.6177	0.1125	0.3450	0.0041	1920	33	1919	17	1911	20	99%
51	395	131	777	0.1352	0.0024	7.4352	0.1349	0.3959	0.0039	2166	31	2165	16	2150	18	99%
52	15	26	30	0.1174	0.0038	5.5211	0.1821	0.3392	0.0042	1916	58	1904	28	1883	20	98%
53	209	135	343	0.1563	0.0031	9.8205	0.1940	0.4525	0.0047	2416	34	2418	18	2406	21	99%
54	69	112	151	0.1123	0.0026	5.1306	0.1219	0.3284	0.0041	1839	42	1841	20	1831	20	99%
55	203	95	303	0.1795	0.0044	12.5131	0.3047	0.5005	0.0061	2650	40	2644	23	2616	26	98%
56	245	442	377	0.1371	0.0039	7.4986	0.2109	0.3936	0.0065	2190	49	2173	25	2139	30	98%
57	14	210	255	0.0506	0.0020	0.2650	0.0105	0.0379	0.0007	220	91	239	8	240	4	99%
58	229	207	337	0.1628	0.0033	10.5508	0.2059	0.4669	0.0043	2485	35	2484	18	2470	19	99%
59	221	179	371	0.1469	0.0027	8.8598	0.1641	0.4351	0.0046	2310	30	2324	17	2329	21	99%
60	54	46	123	0.1222	0.0022	6.2166	0.1730	0.3631	0.0067	1989	27	2007	24	1997	32	99%
61	134	214	279	0.1125	0.0018	5.1407	0.0824	0.3302	0.0029	1840	29	1843	14	1839	14	99%
62	65	51	106	0.1583	0.0025	10.1500	0.1868	0.4643	0.0060	2439	27	2449	17	2459	26	99%
63	64	62	176	0.1123	0.0033	4.3055	0.1185	0.2775	0.0041	1839	52	1694	23	1579	21	92%
64	184	132	274	0.1638	0.0025	10.8860	0.1886	0.4809	0.0054	2496	26	2513	16	2531	24	99%
65	204	189	338	0.1504	0.0022	9.0793	0.1482	0.4370	0.0048	2350	25	2346	15	2337	22	99%
66	171	249	611	0.0855	0.0013	2.6479	0.0575	0.2242	0.0044	1328	29	1314	16	1304	23	99%
67	17	171	319	0.0516	0.0015	0.3016	0.0086	0.0426	0.0005	333	60	268	7	269	3	99%
68	6	50	109	0.0522	0.0024	0.2962	0.0132	0.0416	0.0008	300	104	263	10	263	5	99%
69	14	188	243	0.0516	0.0023	0.2916	0.0136	0.0408	0.0004	333	100	260	11	258	3	99%
70	36	39	54	0.1614	0.0025	10.5088	0.1818	0.4717	0.0051	2470	26	2481	16	2491	22	99%
71	44	93	114	0.1006	0.0017	3.9404	0.0788	0.2836	0.0039	1635	31	1622	16	1610	20	99%
72	20	22	35	0.1421	0.0059	8.0971	0.3333	0.4133	0.0078	2254	72	2242	37	2230	36	99%
73	7	74	103	0.0539	0.0036	0.3806	0.0243	0.0516	0.0015	369	156	327	18	325	9	99%
74	44	54	70	0.1558	0.0022	9.9388	0.2034	0.4602	0.0069	2410	24	2429	19	2440	31	99%
75	132	223	171	0.1649	0.0024	10.8707	0.1661	0.4768	0.0050	2506	24	2512	14	2513	22	99%
76	207	107	465	0.1214	0.0016	5.9429	0.0805	0.3543	0.0032	1977	23	1968	12	1955	15	99%
77	18	320	300	0.0521	0.0017	0.2923	0.0093	0.0410	0.0006	300	74	260	7	259	4	99%
78	106	102	157	0.1677	0.0023	11.2668	0.2135	0.4853	0.0068	2535	17	2545	18	2550	29	99%
79	14	218	223	0.0511	0.0019	0.3094	0.0117	0.0437	0.0005	256	81	274	9	276	3	99%
80	121	112	271	0.1171	0.0017	5.5104	0.0915	0.3399	0.0031	1913	26	1902	14	1886	15	99%

Table 4. U-Pb isotope test results of detrital zircon from the Zhiluo Formation sandstone (G36-1) in study area.

Point No.	Content ($\times 10^{-6}$)			Isotope Ratio						Age (Ma)						
	Pb	Th	U	$^{207}\text{Pb}/^{206}\text{Pb}$	1σ	$^{207}\text{Pb}/^{235}\text{U}$	1σ	$^{206}\text{Pb}/^{238}\text{U}$	1σ	$^{207}\text{Pb}/^{206}\text{Pb}$	1σ	$^{207}\text{Pb}/^{235}\text{U}$	1σ	$^{206}\text{Pb}/^{238}\text{U}$	1σ	Concordia
01	488	176	840	0.1571	0.0023	9.8159	0.2343	0.4515	0.0079	2424	25	2418	22	2402	35	99%
02	24	44	54	0.1105	0.0021	4.8660	0.1005	0.3193	0.0040	1809	33	1796	17	1786	20	99%
03	78	65	180	0.1198	0.0016	5.8288	0.0877	0.3530	0.0042	1954	24	1951	13	1949	20	99%
04	20	39	47	0.1080	0.0019	4.7050	0.1024	0.3153	0.0044	1766	33	1768	18	1767	22	99%
05	36	48	79	0.1172	0.0017	5.6549	0.0960	0.3490	0.0036	1915	27	1925	15	1930	17	99%
06	11	33	23	0.1100	0.0029	4.8790	0.1385	0.3210	0.0043	1811	48	1799	24	1795	21	99%
07	128	35	301	0.1227	0.0016	6.2534	0.1137	0.3681	0.0049	1995	24	2012	16	2021	23	99%
08	73	114	171	0.1101	0.0016	5.0067	0.0946	0.3284	0.0043	1811	26	1820	16	1830	21	99%
09	26	270	534	0.0510	0.0011	0.2904	0.0075	0.0412	0.0006	243	55	259	6	260	4	99%
10	4	101	66	0.0515	0.0025	0.3205	0.0160	0.0451	0.0007	261	111	282	12	284	4	99%
11	167	188	276	0.1545	0.0023	9.4657	0.1705	0.4432	0.0057	2398	25	2384	17	2365	26	99%
12	6	101	170	0.0503	0.0027	0.2004	0.0102	0.0292	0.0004	206	126	185	9	186	2	99%
13	126	213	264	0.1197	0.0015	5.8538	0.0882	0.3541	0.0037	1952	22	1954	13	1954	18	99%
14	22	43	48	0.1144	0.0022	5.2557	0.1169	0.3329	0.0046	1872	34	1862	19	1853	22	99%
15	164	192	257	0.1607	0.0021	10.5018	0.1902	0.4733	0.0064	2465	22	2480	17	2498	28	99%
16	5	49	90	0.0521	0.0023	0.3235	0.0153	0.0449	0.0008	287	99	285	12	283	5	99%
17	156	129	253	0.1606	0.0020	10.1918	0.1518	0.4597	0.0045	2462	20	2452	14	2438	20	99%
18	18	34	39	0.1154	0.0020	5.3586	0.1112	0.3374	0.0048	1887	31	1878	18	1874	23	99%
19	72	99	156	0.1194	0.0016	5.8072	0.1011	0.3521	0.0042	1948	24	1947	15	1944	20	99%
20	137	344	291	0.1118	0.0013	5.0658	0.0811	0.3281	0.0039	1829	20	1830	14	1829	19	99%
21	42	33	63	0.1692	0.0029	11.0568	0.2192	0.4755	0.0081	2550	34	2528	19	2507	36	99%
22	23	62	47	0.1132	0.0020	5.0877	0.1126	0.3260	0.0048	1852	32	1834	19	1819	23	99%
23	13	130	245	0.0520	0.0012	0.3253	0.0090	0.0454	0.0008	287	54	286	7	286	5	99%
24	39	66	90	0.1120	0.0018	5.0770	0.1042	0.3286	0.0046	1832	29	1832	17	1831	22	99%
25	86	78	193	0.1210	0.0016	6.0484	0.1181	0.3620	0.0055	1972	24	1983	17	1992	26	99%
26	15	36	33	0.1137	0.0022	5.1126	0.1132	0.3264	0.0047	1859	35	1838	19	1821	23	99%
27	18	47	36	0.1131	0.0023	5.0581	0.1168	0.3258	0.0054	1850	37	1829	20	1818	26	99%
28	441	396	692	0.1638	0.0018	10.3949	0.1518	0.4593	0.0045	2495	19	2471	14	2436	20	98%
29	124	154	323	0.1079	0.0014	4.4603	0.0735	0.2995	0.0033	1765	24	1724	14	1689	16	97%
30	42	65	113	0.1010	0.0015	3.9510	0.0775	0.2836	0.0038	1643	29	1624	16	1609	19	99%
31	29	13	48	0.1674	0.0026	10.6014	0.2031	0.4596	0.0062	2532	26	2489	18	2438	27	97%
32	18	65	34	0.1094	0.0025	4.7339	0.1207	0.3142	0.0041	1791	42	1773	21	1761	20	99%
33	23	26	43	0.1356	0.0022	7.3477	0.1412	0.3934	0.0047	2172	34	2155	17	2139	22	99%
34	70	147	163	0.1040	0.0014	4.2115	0.0679	0.2939	0.0030	1698	25	1676	13	1661	15	99%
35	9	111	160	0.0512	0.0027	0.2994	0.0160	0.0425	0.0005	256	122	266	12	268	3	99%
36	124	176	246	0.1245	0.0017	6.4151	0.1630	0.3701	0.0065	2022	29	2034	22	2030	31	99%
37	176	229	269	0.1667	0.0019	11.0306	0.2273	0.4801	0.0084	2524	19	2526	19	2528	37	99%
38	33	69	43	0.1661	0.0025	10.9145	0.2212	0.4767	0.0067	2518	24	2516	19	2513	29	99%
39	20	43	40	0.1145	0.0021	5.3444	0.1173	0.3394	0.0048	1872	33	1876	19	1884	23	99%
40	2	33	57	0.0510	0.0045	0.1960	0.0162	0.0283	0.0007	243	199	182	14	180	5	99%
41	23	468	281	0.0530	0.0012	0.3703	0.0096	0.0506	0.0006	328	56	320	7	318	4	99%

Table 4. Cont.

Point No.	Content ($\times 10^{-6}$)			Isotope Ratio						Age (Ma)						
	Pb	Th	U	$^{207}\text{Pb}/^{206}\text{Pb}$	1σ	$^{207}\text{Pb}/^{235}\text{U}$	1σ	$^{206}\text{Pb}/^{238}\text{U}$	1σ	$^{207}\text{Pb}/^{206}\text{Pb}$	1σ	$^{207}\text{Pb}/^{235}\text{U}$	1σ	$^{206}\text{Pb}/^{238}\text{U}$	1σ	Concordia
42	35	686	516	0.0520	0.0013	0.3296	0.0091	0.0459	0.0006	287	56	289	7	289	4	99%
43	12	16	18	0.1551	0.0031	9.6243	0.2091	0.4506	0.0058	2403	34	2399	20	2398	26	99%
44	10	74	203	0.0514	0.0019	0.2973	0.0112	0.0421	0.0006	257	87	264	9	266	4	99%
45	6	92	101	0.0519	0.0018	0.3154	0.0112	0.0445	0.0007	280	84	278	9	281	4	99%
46	49	74	116	0.1102	0.0016	4.9360	0.0877	0.3246	0.0042	1803	26	1808	15	1812	21	99%
47	7	85	126	0.0523	0.0016	0.3318	0.0108	0.0461	0.0007	302	70	291	8	290	4	99%
48	19	150	388	0.0510	0.0011	0.2986	0.0079	0.0424	0.0007	239	56	265	6	268	4	99%
49	57	28	87	0.1828	0.0025	12.7917	0.2656	0.5061	0.0082	2680	23	2664	20	2640	35	99%
50	31	410	428	0.0531	0.0014	0.3774	0.0103	0.0514	0.0006	332	59	325	8	323	4	99%
51	58	109	118	0.1198	0.0017	5.7565	0.0924	0.3478	0.0035	1953	30	1940	14	1924	17	99%
52	74	76	107	0.1706	0.0020	11.3943	0.1606	0.4835	0.0049	2565	20	2556	13	2542	21	99%
53	79	22	182	0.1234	0.0016	6.1875	0.1238	0.3624	0.0058	2006	23	2003	18	1994	28	99%
54	40	56	82	0.1254	0.0018	6.3719	0.1115	0.3679	0.0044	2035	26	2028	15	2020	21	99%
55	54	67	119	0.1213	0.0017	5.9798	0.1028	0.3565	0.0042	1976	58	1973	15	1965	20	99%
56	296	240	459	0.1669	0.0020	11.0846	0.1649	0.4800	0.0047	2527	20	2530	14	2527	20	99%
57	151	262	231	0.1542	0.0020	9.7970	0.1718	0.4600	0.0062	2394	21	2416	16	2439	27	99%
58	15	47	26	0.1185	0.0031	5.7141	0.1550	0.3500	0.0048	1944	46	1934	23	1935	23	99%
59	159	207	235	0.1644	0.0022	10.6572	0.2133	0.4691	0.0073	2502	22	2494	19	2479	32	99%
60	78	98	118	0.1626	0.0020	10.4680	0.1578	0.4667	0.0052	2483	21	2477	14	2469	23	99%
61	28	70	60	0.1138	0.0020	5.1783	0.1040	0.3301	0.0038	1861	33	1849	17	1839	18	99%
62	36	766	509	0.0526	0.0009	0.3386	0.0069	0.0467	0.0006	309	8	296	5	294	3	99%
63	17	198	324	0.0514	0.0012	0.2968	0.0078	0.0420	0.0006	257	49	264	6	265	4	99%
64	23	69	47	0.1137	0.0022	5.1604	0.1237	0.3292	0.0051	1861	35	1846	20	1834	25	99%
65	120	75	279	0.1207	0.0016	6.0511	0.1116	0.3635	0.0052	1969	24	1983	16	1999	24	99%
66	45	48	76	0.1519	0.0020	9.2625	0.1777	0.4419	0.0062	2369	23	2364	18	2359	28	99%
67	12	80	137	0.0551	0.0014	0.5395	0.0162	0.0710	0.0012	417	56	438	11	442	7	99%
68	146	124	244	0.1589	0.0018	9.9790	0.1539	0.4553	0.0049	2444	19	2433	14	2419	22	99%
69	305	573	621	0.1177	0.0014	5.5608	0.0949	0.3422	0.0040	1921	20	1910	15	1897	19	99%
70	22	196	442	0.0522	0.0011	0.3031	0.0069	0.0423	0.0005	295	44	269	5	267	3	99%
71	14	172	255	0.0518	0.0014	0.3066	0.0086	0.0432	0.0006	276	66	272	7	272	4	99%
72	14	97	246	0.0528	0.0019	0.3411	0.0121	0.0472	0.0007	320	80	298	9	297	4	99%
73	41	98	53	0.1633	0.0025	10.5875	0.2052	0.4701	0.0058	2490	26	2488	18	2484	25	99%
74	17	45	35	0.1138	0.0024	5.1327	0.1189	0.3286	0.0048	1861	33	1842	20	1832	23	99%
75	4	40	14	0.1164	0.0044	3.5185	0.1692	0.2170	0.0051	1902	69	1531	38	1266	27	81%
76	391	498	607	0.1542	0.0018	9.6251	0.1452	0.4531	0.0051	2392	20	2400	14	2409	23	99%
77	61	58	138	0.1216	0.0015	5.9852	0.1006	0.3572	0.0043	1980	22	1974	15	1969	20	99%
78	52	91	101	0.1248	0.0016	6.3038	0.1180	0.3672	0.0056	2026	24	2019	16	2016	27	99%
79	24	48	62	0.1026	0.0018	4.1261	0.0870	0.2925	0.0041	1672	33	1659	17	1654	21	99%
80	24	591	297	0.0532	0.0012	0.3494	0.0085	0.0479	0.0006	345	52	304	6	302	4	99%
81	24	46	54	0.1133	0.0020	5.0858	0.1104	0.3253	0.0041	1854	32	1834	18	1816	20	99%
82	53	44	82	0.1726	0.0023	11.6939	0.2096	0.4912	0.0066	2584	23	2580	17	2576	29	99%

Table 4. Cont.

Point No.	Content ($\times 10^{-6}$)			Isotope Ratio						Age (Ma)						
	Pb	Th	U	$^{207}\text{Pb}/^{206}\text{Pb}$	1 σ	$^{207}\text{Pb}/^{235}\text{U}$	1 σ	$^{206}\text{Pb}/^{238}\text{U}$	1 σ	$^{207}\text{Pb}/^{206}\text{Pb}$	1 σ	$^{207}\text{Pb}/^{235}\text{U}$	1 σ	$^{206}\text{Pb}/^{238}\text{U}$	1 σ	Concordia
83	12	166	173	0.0526	0.0013	0.3573	0.0098	0.0493	0.0007	309	56	310	7	310	4	99%
84	22	8	50	0.1238	0.0018	6.2817	0.1255	0.3677	0.0056	2013	27	2016	18	2019	26	99%
85	9	16	22	0.1070	0.0030	4.5098	0.1313	0.3062	0.0047	1750	50	1733	24	1722	23	99%
86	222	518	232	0.1893	0.0032	13.6934	0.3950	0.5210	0.0125	2736	28	2729	27	2703	53	99%
87	15	34	30	0.1137	0.0023	5.2162	0.1270	0.3321	0.0049	1859	37	1855	21	1848	24	99%
88	50	156	95	0.1125	0.0018	5.0032	0.0911	0.3223	0.0044	1840	28	1820	15	1801	21	98%
89	16	160	288	0.0515	0.0013	0.3023	0.0082	0.0426	0.0006	261	53	268	6	269	4	99%
90	27	281	337	0.0540	0.0028	0.4282	0.0209	0.0576	0.0008	372	115	362	15	361	5	99%
91	231	276	423	0.1435	0.0016	8.2821	0.1448	0.4174	0.0062	2270	25	2262	16	2249	28	99%
92	37	45	82	0.1165	0.0022	5.4617	0.1264	0.3385	0.0046	1906	34	1895	20	1879	22	99%
93	20	128	193	0.0564	0.0018	0.6215	0.0210	0.0796	0.0009	478	103	491	13	493	5	99%
94	32	57	72	0.1158	0.0020	5.3692	0.1117	0.3350	0.0042	1894	31	1880	18	1863	20	99%
95	45	59	73	0.1532	0.0023	9.3550	0.1780	0.4417	0.0056	2383	21	2373	18	2358	25	99%

Table 5. U-Pb isotope test results of detrital zircon from the Zhiluo Formation sandstone (G41-1) in study area.

Point No.	Content ($\times 10^{-6}$)			Isotope Ratio						Age (Ma)						
	Pb	Th	U	$^{207}\text{Pb}/^{206}\text{Pb}$	1 σ	$^{207}\text{Pb}/^{235}\text{U}$	1 σ	$^{206}\text{Pb}/^{238}\text{U}$	1 σ	$^{207}\text{Pb}/^{206}\text{Pb}$	1 σ	$^{207}\text{Pb}/^{235}\text{U}$	1 σ	$^{206}\text{Pb}/^{238}\text{U}$	1 σ	Concordia
01	134	121	255	0.1333	0.0020	7.2283	0.1221	0.3918	0.0045	2142	26	2140	15	2131	21	99%
02	153	49	252	0.1686	0.0023	11.2753	0.2067	0.4820	0.0061	2544	23	2546	17	2536	26	99%
03	90	153	154	0.1339	0.0019	7.3196	0.1148	0.3949	0.0037	2150	24	2151	14	2146	17	99%
04	19	359	240	0.0520	0.0017	0.3318	0.0108	0.0462	0.0005	283	79	291	8	291	3	99%
05	61	66	108	0.1332	0.0021	7.3286	0.1275	0.3974	0.0036	2143	28	2152	16	2157	17	99%
06	101	36	232	0.1154	0.0017	5.5290	0.1070	0.3478	0.0058	1887	32	1905	17	1924	28	99%
07	2	14	28	0.0591	0.0064	0.3865	0.0320	0.0533	0.0012	572	237	332	23	335	7	99%
08	7	99	118	0.0521	0.0026	0.2990	0.0154	0.0418	0.0007	300	149	266	12	264	4	99%
09	5	47	85	0.0544	0.0027	0.3717	0.0183	0.0505	0.0010	387	109	321	14	318	6	99%
10	88	137	186	0.1139	0.0034	5.1450	0.1368	0.3275	0.0051	1862	53	1844	23	1826	25	99%
11	249	290	538	0.1179	0.0014	5.6079	0.0811	0.3442	0.0033	1924	22	1917	13	1907	16	99%
12	165	143	257	0.1594	0.0035	9.8932	0.1711	0.4493	0.0066	2450	37	2425	16	2392	30	98%
13	69	29	101	0.1757	0.0048	11.9957	0.3162	0.4945	0.0075	2613	44	2604	25	2590	32	99%
14	199	98	463	0.1185	0.0017	5.5671	0.0904	0.3395	0.0034	1944	26	1911	14	1884	16	98%
15	202	222	295	0.1667	0.0023	11.1095	0.2052	0.4816	0.0064	2525	23	2532	17	2534	28	99%
16	6	14	12	0.1135	0.0043	4.9444	0.1848	0.3193	0.0050	1857	69	1810	32	1786	24	98%
17	23	53	41	0.1202	0.0038	5.6912	0.1746	0.3443	0.0047	1958	56	1930	27	1907	23	98%

Table 5. Cont.

Point No.	Content ($\times 10^{-6}$)				Isotope Ratio				Age (Ma)				Concordia			
	Pb	Th	U	$^{207}\text{Pb}/^{206}\text{Pb}$	1σ	$^{207}\text{Pb}/^{235}\text{U}$	1σ	$^{206}\text{Pb}/^{238}\text{U}$	1σ	$^{207}\text{Pb}/^{206}\text{Pb}$	1σ	$^{207}\text{Pb}/^{235}\text{U}$	1σ	$^{206}\text{Pb}/^{238}\text{U}$	1σ	
18	55	73	70	0.1790	0.0039	12.2672	0.2812	0.4951	0.0052	2644	36	2625	22	2593	23	98%
19	68	77	108	0.1519	0.0022	9.1758	0.1576	0.4365	0.0047	2368	25	2356	16	2335	21	99%
20	23	38	48	0.1149	0.0055	5.1782	0.2583	0.3260	0.0069	1880	85	1849	42	1819	33	98%
21	28	72	88	0.0876	0.0016	2.7733	0.0562	0.2291	0.0026	1374	35	1348	15	1330	14	98%
22	165	52	261	0.1714	0.0024	11.2825	0.1890	0.4759	0.0054	2571	24	2547	16	2509	24	98%
23	41	62	55	0.1679	0.0028	10.7871	0.2178	0.4637	0.0058	2537	28	2505	19	2456	25	98%
24	37	49	85	0.1090	0.0042	4.7631	0.1968	0.3153	0.0043	1783	70	1778	35	1767	21	99%
25	299	295	418	0.1701	0.0026	11.2625	0.1907	0.4783	0.0050	2558	25	2545	16	2520	22	99%
26	40	51	56	0.1621	0.0042	10.3666	0.2620	0.4634	0.0060	2477	44	2468	23	2455	27	99%
27	60	71	91	0.1543	0.0052	9.5164	0.2509	0.4478	0.0071	2394	57	2389	24	2385	31	99%
28	166	160	249	0.1584	0.0023	9.9869	0.1508	0.4558	0.0039	2439	25	2434	14	2421	17	99%
29	44	92	91	0.1106	0.0019	4.9417	0.1014	0.3224	0.0036	1810	27	1809	17	1802	18	99%
30	123	48	298	0.1120	0.0022	5.0586	0.1113	0.3264	0.0039	1832	69	1829	19	1821	19	99%
31	182	349	350	0.1184	0.0016	5.8058	0.0935	0.3544	0.0036	1932	24	1947	14	1956	17	99%
32	16	33	31	0.1151	0.0031	5.2231	0.1407	0.3310	0.0045	1881	48	1856	23	1843	22	99%
33	152	196	243	0.1547	0.0082	9.1262	0.3445	0.4259	0.0073	2399	90	2351	35	2287	33	97%
34	168	56	381	0.1209	0.0017	5.9643	0.1105	0.3564	0.0052	1970	25	1971	16	1965	25	99%
35	45	49	56	0.1771	0.0030	12.4666	0.3502	0.5053	0.0110	2628	28	2640	26	2636	47	99%
36	53	62	90	0.1442	0.0022	8.4019	0.1616	0.4203	0.0050	2280	26	2275	18	2262	23	99%
37	358	555	2006	0.1411	0.0018	3.0337	0.0739	0.1553	0.0033	2243	23	1416	49	931	49	58%
38	75	141	170	0.1118	0.0018	5.0270	0.0944	0.3250	0.0035	1829	30	1824	16	1814	17	99%
39	56	52	112	0.1225	0.0042	6.2902	0.2412	0.3702	0.0053	1994	61	2017	34	2030	25	99%
40	28	297	432	0.0532	0.0012	0.3682	0.0087	0.0501	0.0006	339	50	318	6	315	4	99%
41	131	41	215	0.1642	0.0026	10.7765	0.1752	0.4734	0.0043	2500	26	2504	15	2499	19	99%
42	109	111	160	0.1690	0.0024	11.3348	0.1975	0.4830	0.0056	2548	24	2551	16	2540	24	99%
43	124	73	193	0.1688	0.0023	11.2730	0.1921	0.4804	0.0055	2546	22	2546	16	2529	24	99%
44	123	206	210	0.1303	0.0064	6.9618	0.3474	0.3842	0.0063	2102	86	2107	44	2096	29	99%
45	190	326	328	0.1316	0.0020	7.2232	0.1357	0.3940	0.0049	2120	27	2139	17	2141	23	99%
46	58	101	85	0.1578	0.0029	9.7556	0.1815	0.4445	0.0045	2433	32	2412	17	2371	20	98%
47	196	169	354	0.1399	0.0026	7.7811	0.1472	0.3992	0.0042	2228	31	2206	17	2165	19	98%
48	182	169	277	0.1559	0.0035	9.8419	0.2247	0.4525	0.0050	2413	38	2420	21	2406	22	99%
49	74	61	114	0.1622	0.0031	10.6696	0.2021	0.4721	0.0047	2479	32	2495	18	2493	21	99%
50	25	11	34	0.1937	0.0036	14.5594	0.2840	0.5404	0.0063	2774	31	2787	19	2785	27	99%
51	131	214	253	0.1132	0.0022	5.5366	0.1822	0.3501	0.0090	1852	35	1906	28	1935	43	98%
52	167	162	253	0.1553	0.0038	10.0653	0.2403	0.4651	0.0049	2405	40	2441	22	2462	22	99%
53	61	119	82	0.1547	0.0028	9.8963	0.1759	0.4602	0.0047	2398	30	2425	16	2441	21	99%
54	166	226	325	0.1211	0.0020	6.1808	0.1026	0.3665	0.0034	1972	29	2002	15	2013	16	99%
55	103	110	213	0.1195	0.0021	6.0702	0.1143	0.3645	0.0040	1950	32	1986	16	2003	19	99%
56	281	404	468	0.1310	0.0052	7.4192	0.2590	0.4069	0.0088	2122	68	2163	31	2201	40	98%
57	251	173	481	0.1355	0.0023	7.8863	0.1359	0.4189	0.0046	2172	35	2218	16	2256	21	98%
58	15	169	234	0.0521	0.0016	0.3608	0.0114	0.0500	0.0009	300	75	313	9	315	5	99%

Table 5. Cont.

Point No.	Content ($\times 10^{-6}$)			Isotope Ratio						Age (Ma)						Concordia
	Pb	Th	U	$^{207}\text{Pb}/^{206}\text{Pb}$	1 σ	$^{207}\text{Pb}/^{235}\text{U}$	1 σ	$^{206}\text{Pb}/^{238}\text{U}$	1 σ	$^{207}\text{Pb}/^{206}\text{Pb}$	1 σ	$^{207}\text{Pb}/^{235}\text{U}$	1 σ	$^{206}\text{Pb}/^{238}\text{U}$	1 σ	
59	5	2	12	0.1218	0.0039	6.2485	0.2048	0.3728	0.0055	1983	58	2011	29	2043	26	98%
60	39	67	90	0.1090	0.0023	5.1806	0.1164	0.3428	0.0042	1784	45	1849	19	1900	20	97%
61	16	122	304	0.0528	0.0043	0.3346	0.0266	0.0457	0.0010	320	187	293	20	288	6	98%
62	19	59	38	0.1096	0.0028	5.1636	0.1419	0.3401	0.0051	1794	46	1847	23	1887	24	97%
63	290	90	494	0.1581	0.0032	10.7580	0.2125	0.4904	0.0050	2436	34	2502	18	2572	22	97%
64	21	37	44	0.1124	0.0031	5.5711	0.1583	0.3573	0.0043	1839	50	1912	24	1969	20	97%
65	188	104	264	0.1989	0.0041	14.8638	0.3076	0.5391	0.0063	2817	34	2807	20	2780	26	99%
66	71	131	160	0.1139	0.0021	5.2068	0.1039	0.3304	0.0042	1863	33	1854	17	1840	20	99%
67	117	74	337	0.1092	0.0030	4.3282	0.1331	0.2857	0.0039	1787	49	1699	25	1620	20	95%
68	117	32	295	0.1170	0.0025	5.4865	0.1118	0.3392	0.0043	1910	39	1898	18	1883	21	99%
69	416	136	918	0.1668	0.0025	8.6891	0.1541	0.3759	0.0044	2528	25	2306	16	2057	21	88%
70	160	166	227	0.1696	0.0027	11.5183	0.2029	0.4900	0.0052	2553	26	2566	17	2571	23	99%
71	178	86	403	0.1232	0.0022	6.0996	0.1193	0.3578	0.0052	2003	31	1990	17	1972	25	99%
72	102	35	249	0.1198	0.0021	6.0216	0.1507	0.3611	0.0062	1954	31	1979	22	1987	29	99%
73	92	52	146	0.1727	0.0027	11.6684	0.2021	0.4877	0.0051	2584	26	2578	16	2561	22	99%
74	113	99	242	0.1201	0.0023	5.8382	0.1149	0.3507	0.0036	1958	33	1952	17	1938	17	99%
75	170	91	244	0.1816	0.0026	12.8460	0.1936	0.5104	0.0043	2668	24	2668	14	2658	18	99%
76	27	44	54	0.1155	0.0028	5.5237	0.1367	0.3448	0.0035	1889	38	1904	21	1910	17	99%
77	115	207	154	0.1574	0.0024	9.9282	0.1625	0.4547	0.0036	2427	26	2428	15	2416	16	99%
78	42	77	79	0.1209	0.0023	6.0092	0.1246	0.3594	0.0044	1969	31	1977	18	1979	21	99%
79	103	101	159	0.1561	0.0024	9.8995	0.1708	0.4578	0.0048	2414	27	2425	16	2430	21	99%
80	21	69	32	0.1280	0.0048	6.6865	0.2840	0.3761	0.0068	2070	98	2071	38	2058	32	99%
81	172	278	361	0.1214	0.0019	6.1170	0.1195	0.3641	0.0048	1976	29	1993	17	2002	23	99%
82	68	45	97	0.1746	0.0030	12.0000	0.2132	0.4971	0.0057	2602	29	2604	17	2601	25	99%
83	68	59	142	0.1244	0.0021	6.3130	0.1201	0.3662	0.0039	2020	31	2020	17	2012	18	99%
84	4	63	64	0.0538	0.0027	0.3179	0.0143	0.0441	0.0007	361	111	280	11	278	4	99%
85	239	98	409	0.1588	0.0022	10.1076	0.1673	0.4589	0.0050	2444	23	2445	15	2435	22	99%
86	26	45	54	0.1146	0.0027	5.3184	0.1300	0.3359	0.0046	1876	43	1872	21	1867	22	99%
87	32	439	466	0.0526	0.0012	0.3486	0.0082	0.0479	0.0005	309	50	304	6	301	3	99%
88	117	27	261	0.1210	0.0023	6.1453	0.1329	0.3662	0.0047	1972	34	1997	19	2011	22	99%

Table 6. U-Pb isotope test results of detrital zircon from the Zhiluo Formation sandstone (G43-1) in study area.

Point No.	Content ($\times 10^{-6}$)			Isotope Ratio						Age (Ma)						Concordia
	Pb	Th	U	$^{207}\text{Pb}/^{206}\text{Pb}$	1 σ	$^{207}\text{Pb}/^{235}\text{U}$	1 σ	$^{206}\text{Pb}/^{238}\text{U}$	1 σ	$^{207}\text{Pb}/^{206}\text{Pb}$	1 σ	$^{207}\text{Pb}/^{235}\text{U}$	1 σ	$^{206}\text{Pb}/^{238}\text{U}$	1 σ	
01	69	78	98	0.1587	0.0023	10.3449	0.1724	0.4713	0.0049	2443	25	2466	16	2489	21	99%
02	154	23	260	0.1534	0.0019	9.6150	0.1318	0.4533	0.0042	2384	21	2399	13	2410	18	99%
03	74	69	122	0.1497	0.0019	9.1027	0.1381	0.4395	0.0046	2343	22	2348	14	2349	21	99%

Table 6. Cont.

Point No.	Content ($\times 10^{-6}$)			Isotope Ratio						Age (Ma)						
	Pb	Th	U	$^{207}\text{Pb}/^{206}\text{Pb}$	1σ	$^{207}\text{Pb}/^{235}\text{U}$	1σ	$^{206}\text{Pb}/^{238}\text{U}$	1σ	$^{207}\text{Pb}/^{206}\text{Pb}$	1σ	$^{207}\text{Pb}/^{235}\text{U}$	1σ	$^{206}\text{Pb}/^{238}\text{U}$	1σ	Concordia
04	137	107	297	0.1192	0.0014	5.9713	0.0928	0.3618	0.0041	1944	21	1972	14	1991	20	99%
05	13	25	24	0.1159	0.0028	5.5273	0.1426	0.3454	0.0042	1894	44	1905	22	1913	20	99%
06	37	288	878	0.1250	0.0020	0.5888	0.0158	0.0340	0.0007	2029	29	470	10	215	5	25%
07	32	470	432	0.0534	0.0020	0.3693	0.0109	0.0502	0.0011	343	88	319	8	316	7	99%
08	119	37	223	0.1431	0.0029	8.2509	0.1783	0.4158	0.0049	2265	35	2259	20	2242	22	99%
09	291	90	476	0.1658	0.0049	10.6827	0.1777	0.4655	0.0131	2517	50	2496	16	2464	57	98%
10	144	43	238	0.1596	0.0053	10.0935	0.2801	0.4577	0.0090	2451	56	2443	26	2430	40	99%
11	50	94	67	0.1687	0.0025	11.1227	0.1966	0.4763	0.0051	2546	25	2533	17	2511	22	99%
12	529	660	652	0.1693	0.0019	11.2791	0.1578	0.4809	0.0045	2551	19	2546	13	2531	19	99%
13	81	75	164	0.1207	0.0018	6.0937	0.0974	0.3645	0.0030	1969	26	1989	14	2004	14	99%
14	23	141	19	0.1202	0.0034	6.0013	0.1817	0.3620	0.0049	1961	50	1976	26	1992	23	99%
15	146	166	209	0.1568	0.0022	9.8306	0.2030	0.4514	0.0060	2421	29	2419	19	2401	27	99%
16	32	58	71	0.1149	0.0019	5.2789	0.1023	0.3328	0.0039	1880	31	1865	17	1852	19	99%
17	37	8	82	0.1233	0.0023	6.3174	0.1255	0.3713	0.0040	2006	32	2021	17	2036	19	99%
18	313	209	500	0.1605	0.0023	10.2578	0.1807	0.4622	0.0045	2461	24	2458	16	2449	20	99%
19	19	51	37	0.1104	0.0031	4.9358	0.1386	0.3259	0.0049	1806	52	1808	24	1818	24	99%
20	227	82	355	0.1741	0.0020	11.7385	0.1524	0.4881	0.0036	2597	14	2584	12	2562	16	99%
21	22	27	41	0.1335	0.0025	7.3044	0.1437	0.3995	0.0055	2144	33	2149	18	2167	25	99%
22	664	507	1490	0.1170	0.0018	5.5966	0.1197	0.3462	0.0068	1911	28	1916	18	1916	33	99%
23	105	77	165	0.1636	0.0025	10.5022	0.1786	0.4653	0.0054	2494	20	2480	16	2463	24	99%
24	149	396	499	0.1097	0.0017	3.1903	0.0576	0.2106	0.0023	1794	27	1455	14	1232	12	83%
25	133	152	202	0.1607	0.0021	10.4623	0.1666	0.4711	0.0048	2463	21	2477	15	2488	21	99%
26	381	895	1447	0.1714	0.0021	4.9535	0.1299	0.2094	0.0050	2569	19	1811	22	1226	27	61%
27	94	134	134	0.1588	0.0038	10.0546	0.2167	0.4595	0.0064	2443	40	2440	20	2437	28	99%
28	144	95	233	0.1597	0.0020	10.3857	0.1619	0.4704	0.0051	2454	21	2470	15	2485	22	99%
29	219	90	387	0.1503	0.0037	9.0866	0.5203	0.4363	0.0152	2350	42	2347	52	2334	68	99%
30	36	48	54	0.1582	0.0024	9.9020	0.1750	0.4529	0.0048	2436	26	2426	16	2408	22	99%
31	171	306	548	0.1449	0.0021	4.3961	0.1658	0.2189	0.0076	2287	30	1712	31	1276	40	70%
32	210	272	302	0.1656	0.0025	10.9060	0.1960	0.4757	0.0056	2514	25	2515	17	2508	24	99%
33	97	95	135	0.1739	0.0029	11.8131	0.1965	0.4915	0.0053	2595	33	2590	16	2577	23	99%
34	219	144	359	0.1591	0.0020	10.0706	0.1513	0.4573	0.0047	2446	26	2441	14	2427	21	99%
35	143	119	279	0.1290	0.0019	6.8017	0.1118	0.3805	0.0037	2085	26	2086	15	2079	18	99%
36	31	16	67	0.1257	0.0019	6.5931	0.1106	0.3799	0.0043	2039	26	2058	15	2076	20	99%
37	71	78	95	0.1812	0.0027	12.9273	0.2124	0.5155	0.0053	2665	24	2674	16	2680	22	99%
38	145	148	262	0.1273	0.0016	6.7579	0.1472	0.3803	0.0060	2061	22	2080	19	2078	28	99%
39	28	394	441	0.0524	0.0012	0.3265	0.0077	0.0453	0.0005	302	49	287	6	285	3	99%
40	54	35	115	0.1201	0.0017	6.0533	0.1098	0.3637	0.0046	1958	25	1984	16	2000	22	99%
41	170	218	481	0.1340	0.0017	4.9028	0.0690	0.2642	0.0022	2150	23	1803	12	1511	11	82%
42	97	102	134	0.1731	0.0023	11.7763	0.1721	0.4917	0.0048	2588	23	2587	14	2578	21	99%
43	212	122	498	0.1176	0.0013	5.6383	0.0749	0.3461	0.0031	1920	20	1922	12	1916	15	99%
44	127	149	208	0.1505	0.0017	9.3482	0.1380	0.4485	0.0048	2352	20	2373	14	2389	21	99%

Table 6. Cont.

Point No.	Content ($\times 10^{-6}$)			Isotope Ratio						Age (Ma)						Concordia
	Pb	Th	U	$^{207}\text{Pb}/^{206}\text{Pb}$	1σ	$^{207}\text{Pb}/^{235}\text{U}$	1σ	$^{206}\text{Pb}/^{238}\text{U}$	1σ	$^{207}\text{Pb}/^{206}\text{Pb}$	1σ	$^{207}\text{Pb}/^{235}\text{U}$	1σ	$^{206}\text{Pb}/^{238}\text{U}$	1σ	Concordia
45	379	291	656	0.1441	0.0018	8.5558	0.1211	0.4285	0.0040	2277	21	2292	13	2299	18	99%
46	21	58	43	0.1092	0.0023	4.8300	0.1045	0.3213	0.0037	1787	43	1790	18	1796	18	99%
47	51	80	73	0.1597	0.0026	10.4376	0.1835	0.4732	0.0052	2454	28	2474	16	2498	23	99%
48	12	121	220	0.0509	0.0015	0.3064	0.0090	0.0435	0.0005	239	69	271	7	275	3	98%
49	104	152	172	0.1362	0.0024	7.6426	0.1585	0.4043	0.0051	2179	30	2190	19	2189	23	99%
50	111	69	166	0.1727	0.0025	12.0059	0.2138	0.5013	0.0061	2584	24	2605	17	2619	26	99%
51	460	122	772	0.1684	0.0025	11.2747	0.1968	0.4824	0.0054	2542	26	2546	16	2538	24	99%
52	255	62	505	0.1309	0.0024	7.3821	0.1819	0.4025	0.0058	2110	33	2159	22	2180	27	99%
53	41	47	61	0.1577	0.0032	9.9268	0.2093	0.4538	0.0049	2431	34	2428	20	2412	22	99%
54	213	285	350	0.1375	0.0030	7.9253	0.1752	0.4154	0.0042	2196	38	2223	20	2239	19	99%
55	8	70	110	0.0508	0.0025	0.3667	0.0186	0.0519	0.0008	232	110	317	14	326	5	97%
56	58	58	83	0.1595	0.0044	10.4545	0.2844	0.4734	0.0060	2450	48	2476	25	2498	26	99%
57	384	215	999	0.1395	0.0032	5.5235	0.1350	0.2854	0.0037	2221	40	1904	21	1618	49	83%
58	97	104	143	0.1640	0.0034	10.5507	0.2581	0.4644	0.0074	2498	35	2484	23	2459	32	98%
59	196	109	474	0.1137	0.0021	5.1768	0.1029	0.3284	0.0035	1861	33	1849	17	1831	17	99%
60	111	94	258	0.1107	0.0020	5.0155	0.0930	0.3269	0.0028	1813	27	1822	16	1823	14	99%
61	46	48	71	0.1625	0.0029	10.2332	0.1963	0.4556	0.0050	2483	35	2456	18	2420	22	98%
62	435	28	1178	0.1335	0.0021	5.4102	0.1050	0.2916	0.0032	2146	27	1886	17	1650	46	86%
63	104	384	742	0.1538	0.0027	2.0650	0.1422	0.0965	0.0063	2389	30	1137	47	594	37	37%
64	25	84	51	0.1074	0.0022	4.6085	0.1045	0.3111	0.0040	1767	38	1751	19	1746	20	99%
65	282	283	463	0.1434	0.0047	8.3858	0.5515	0.4216	0.0159	2269	57	2274	60	2268	72	99%
66	24	52	47	0.1124	0.0020	5.1665	0.0998	0.3336	0.0041	1839	33	1847	16	1856	20	99%
67	97	49	226	0.1197	0.0016	5.7717	0.1163	0.3484	0.0054	1954	24	1942	17	1927	26	99%
68	76	141	103	0.1548	0.0032	9.5403	0.1896	0.4461	0.0051	2400	35	2391	18	2378	23	99%
69	117	122	190	0.1544	0.0020	9.6092	0.1526	0.4498	0.0050	2395	22	2398	15	2394	22	99%
70	25	51	54	0.1112	0.0020	5.0086	0.0954	0.3272	0.0039	1820	32	1821	16	1825	19	99%
71	104	112	161	0.1642	0.0023	10.9465	0.2019	0.4817	0.0066	2499	23	2519	17	2534	29	99%
72	275	205	398	0.1757	0.0024	12.1544	0.2016	0.4990	0.0054	2613	23	2616	16	2610	23	99%
73	256	287	392	0.1593	0.0054	10.0735	0.3990	0.4559	0.0061	2448	57	2442	37	2421	27	99%
74	100	87	163	0.1593	0.0020	10.1826	0.1704	0.4616	0.0060	2448	21	2452	16	2447	26	99%
75	127	129	191	0.1659	0.0020	11.0626	0.1810	0.4804	0.0055	2517	20	2528	15	2529	24	99%
76	96	96	212	0.1218	0.0018	6.0450	0.1296	0.3589	0.0066	1983	21	1982	19	1977	32	99%
77	81	263	133	0.1205	0.0018	6.0735	0.1074	0.3647	0.0046	1965	27	1986	15	2005	22	99%
78	164	196	289	0.1378	0.0024	7.8449	0.1617	0.4104	0.0057	2211	30	2213	19	2217	26	99%
79	163	446	283	0.1187	0.0017	5.8080	0.0908	0.3533	0.0036	1937	25	1948	14	1950	17	99%
80	20	57	38	0.1099	0.0028	4.9793	0.1357	0.3285	0.0047	1798	47	1816	23	1831	23	99%

Tables 3–6 uncertainty of 1 sigma.

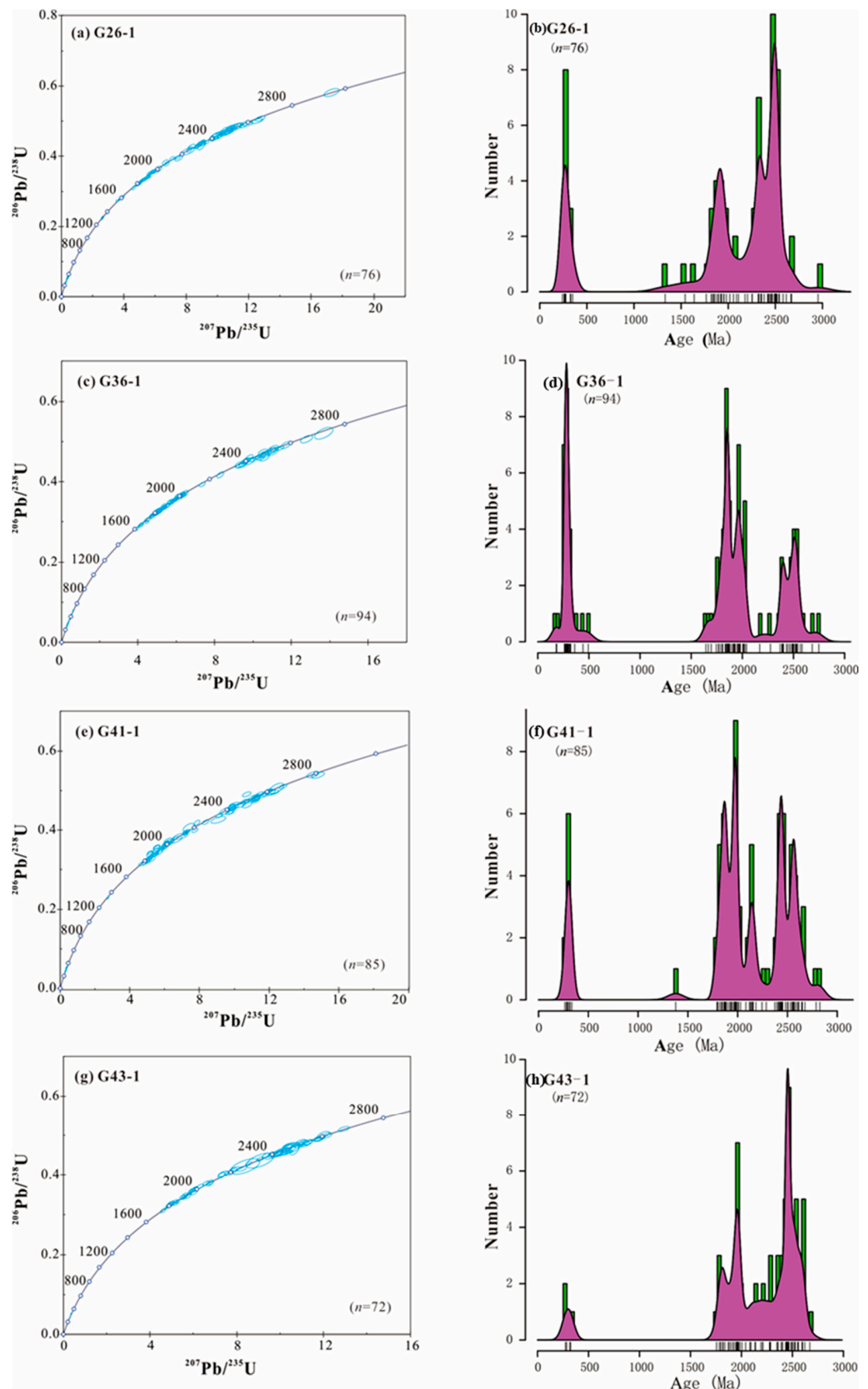


Figure 6. Concordia curves and age spectrum of detrital zircons of the sandstones (G26-1 (a,b), G36-1 (c,d), G41-1 (e,f) and G43-1 (g,h)) from the Zhiluo Formation in the study area (after [23]).

5. Discussion

5.1. Geochemical Characteristics and Tectonic Setting of Host Rocks

On the FeO-MgO-Al₂O₃ diagram [24], the source rocks of the Zhiluo Formation sandstones generally fall into the active continental margin or island-arc settings (Figure 7). In terms of trace element compositions, these sandstones are enriched in LILEs and are strongly depleted in HFSEs (Figure 3). This further suggests that the source rocks of these sandstones may have been formed in typical subduction-related settings. We, therefore, conclude that the source rocks of the Zhiluo Formation in the Daying–Tarangaole–Nalinggou area were formed in island-arc or active continental margin settings.

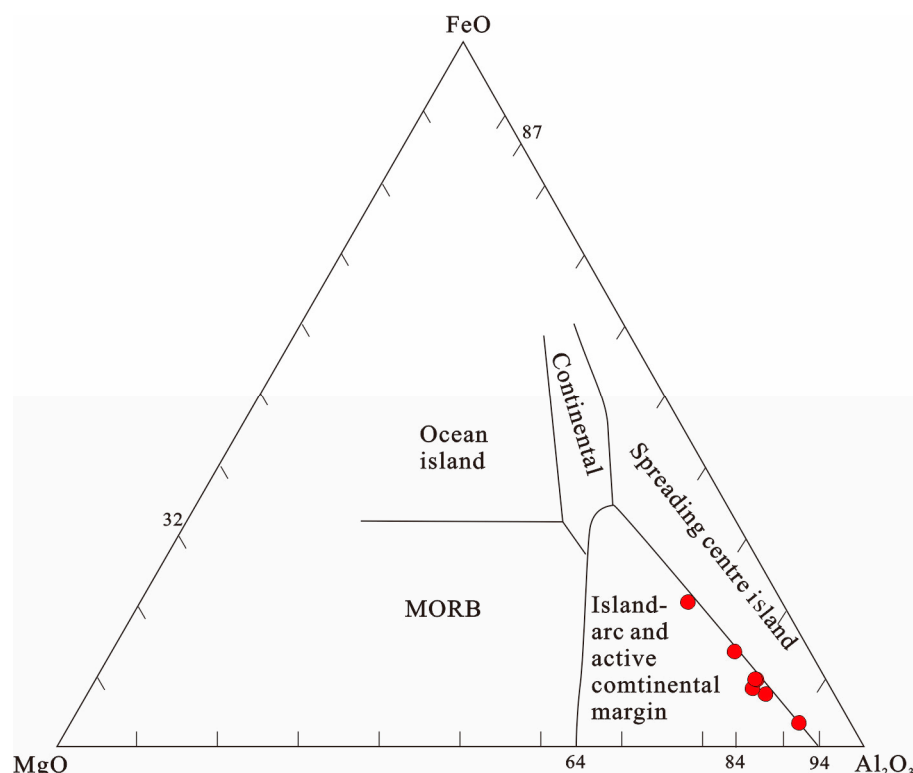


Figure 7. The FeO-MgO-Al₂O₃ discrimination diagram for sandstones samples from the Zhiluo Formation (after [24]).

5.2. Composition of Heavy Mineral and Implications for U Mineralization

Based on the statistical analysis on the composition of heavy minerals for the Zhiluo Formation sandstones, there is no obvious difference for the associations of stable heavy minerals among the three uranium deposits. The content of ilmenite is slightly decreased in some boreholes due to the changing of surface hydrodynamic conditions during the sedimentary processes. From the comparison of the heavy mineral contents (Figure 4), the individual relative enrichment zone can be divided into pyrite and hematite, reflecting that under the same source background, the late oxidation-reduction may have generated some authigenic heavy minerals. Although they may not indicate the source rocks of the material, they can identify the paleo-oxidation-reduction environment, which plays a certain role in indicating the spatial positioning of uranium reservoirs. The pyrite enrichment area represents the dominant zones for reducing fluids, whereas the hematite enrichment area represents the dominant zone for oxidizing fluids. Some pyrite overlaps with the limonite enrichment area, which is considered the oxidation-reduction barrier, a favorable location of U prospection.

5.3. Spatial–Temporal Constraints on the Source Rocks

Compared with the age spectrum of the neighboring areas, the age peaks (i.e., ~260 Ma, ~1850 Ma and ~2450 Ma) (Figure 6) of detrital zircons from the Tarangaole uranium deposit are highly similar to that of the Daqingshan–Ula, Yin and Wolf mountains located at the northern edge of the basin [2,8,9,25]. The Precambrian high-grade metamorphic complex distributed among the Daqing–Ula Mountains is an important part of the khondalite belt on the northern margin of the North China Craton (NCC). It is mainly composed of the Archean Xinghe Rock Group gneiss series (basement reconstructed rock series: 1950~1850 Ma, 2500~2450 Ma), the Paleoproterozoic khondalite series, the (perilla) granitic gneiss–diorite gneiss and the Paleoproterozoic mafic gneiss, the plagioclase amphibole [26]. The metamorphic events are related to the Paleoproterozoic subduction-collision dynamics between the Yinshan Massif and the Ordos Massif on the northern margin of the NCC [27]. The gneiss, granulite, khondalite series and late Paleozoic intermediate and acidic intrusive rocks in these mountains are proposed to be the main sources for sandstones in the Zhiluo Formation [2].

The age peaks of ~1850 Ma and ~2450 Ma are consistent with the two tectonic thermal events in the northern margin of the North China Craton [28] and the age peak of ~260 Ma may record the rapid subduction event of the Paleo-Asian Ocean beneath the northern margin of the North China Craton, respectively [29].

5.4. Origin of Uranium in the Zhiluo Formation

Previous studies have shown that the late Paleozoic granites in the northern Ordos Basin (i.e., source area) are highly enriched in uranium [8], e.g., the ~328 Ma Dahuabei pluton in the Ula Mountain has an average uranium content of 5.16 ppm [30] and the 253~254 Ma Chaganhua Mo-bearing granite in the eastern Wolf Mountain contains a uranium content of 5.2~20.8 ppm [31]. These magmatic rocks were yielded in the source area of the Zhiluo Formation and it can be inferred that the uranium-abnormal properties of the Middle Jurassic Zhiluo Formation sandstones may have been caused by these late Paleozoic acidic uranium-rich magmatic rocks (Figure 8).

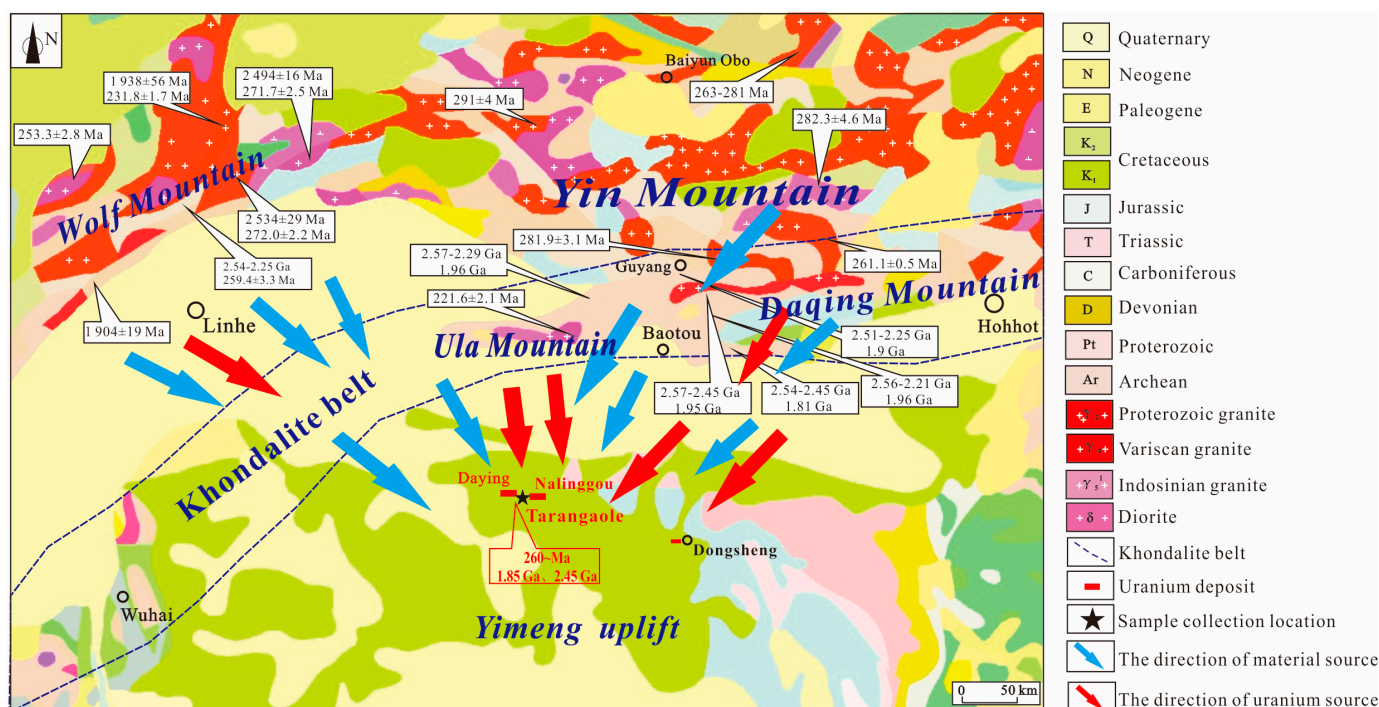


Figure 8. Schematic diagram for the source of sediments and uranium in the Zhiluo Formation, northern Ordos Basin (modified after [2]; the age of magmatic rocks are from [9]).

During the Middle Jurassic, the widely distributed, late Paleozoic uranium-rich intermediate and acidic magmatic rocks in the Ula–Daqing and Wolf mountains along the northern Ordos Basin may have suffered strong uplift and erosion processes [3]. The paleowater flow would carry abundant sediment supplies and the surface water would facilitate the migration of uranium (+6 U) into the basin. During the later reduction stage, the uranium is restored as U ore (+4U) by reducers like pyrite, coal and other organic matter [32].

As a product of the Paleo-Asian Ocean’s evolution, these Carboniferous–Permian uranium-rich intermediate and acidic magmatic rocks are mainly distributed along the northern margin of the North China Craton. As the evolution of these granites directly controls the development of uranium-rich sandstones, the distribution of these granites can be used as a valuable index for the prediction and evaluation of potential uranium resources in the Ordos basin [33].

6. Conclusions

1. Lithogeochemical features indicate that the source rocks of the Zhiluo Formation sandstones may have been formed in island arcs or active continental margins.
2. Heavy mineral assemblage shows that the sedimentary sources of the Zhiluo Formation are mainly from intermediate and acidic magmatic rocks with minor metamorphic rocks. The source areas are located in the northern part of the Ordos Basin, the Ula–Daqing Mountains and the eastern area of the Wolf Mountain.
3. Detrital zircons from the Zhiluo Formation sandstones show three age peaks, i.e., ~2450 Ma, ~1850 Ma and ~260 Ma, which appear to be related to two phases of Paleoproterozoic tectonic thermal events and the rapid subduction of the Paleo-Asian Ocean during the Early Carboniferous–Middle Permian, respectively.
4. The late Paleozoic uranium-rich magmatic rocks successively provide uranium for the Zhiluo Formation sandstones.

Author Contributions: Formal analysis, Q.Z.; Supervision, C.-J.X. and J.-W.Y.; Writing—original draft, G.-Y.L.; Writing—review and editing, X.-B.Z. All authors have read and agreed to the published version of the manuscript.

Funding: This work was financially supported by the National Natural Science Foundation of China (92162212), China Scholarship Council (No. 202308570015), the Geological Survey Project of the China Geological Survey (12120113057300; DD20160129; DD20160014; DD20160039; DD20190119; DD20230027) and the Scientific Research and Technology Development Project of PetroChina Changqing Oilfield Company (2022DJ0611).

Data Availability Statement: Data is contained within the article.

Conflicts of Interest: The authors declare no conflicts of interest.

References

1. Liu, C.Y.; Zhao, H.G.; Gui, X.J.; Yue, L.P.; Zhao, J.F.; Wang, J.Q. Space- Time coordinate of the evolution and reformation and mineralization response in Ordos Basin. *Acta Geol. Sin.* **2006**, *80*, 617–638. (In Chinese with English abstract)
2. Yu, R.A.; Sima, X.Z.; Jin, R.S.; Miao, P.S.; Peng, S.L. Discovery of a large-size uranium deposit in Northeast Ordos Basin. *Geol. China* **2020**, *47*, 883–884.
3. Zhu, Q.; Yu, R.A.; Feng, X.X.; Li, J.G.; SiMa, X.Z.; Tang, C.; Xu, Z.L.; Liu, X.X.; Si, Q.H.; Li, G.Y.; et al. Mineralogy, geochemistry, and fluid action process of uranium deposits in the Zhiluo Formation, Ordos Basin, China. *Ore Geol. Rev.* **2019**, *111*, 102984. [[CrossRef](#)]
4. Zhu, Q.; Wu, Y.; Wen, S.B.; Wang, Y.; Li, G.Y.; Si, Q.H.; Zhao, H.L. Analysis and comparative research on metallogenetic geo-logical characteristics of sandstone-type uranium deposits between Zhiluo Formation and Luohe Formation in Ordos Basin. *North China Geol.* **2022**, *45*, 28–37.
5. Chen, L.L.; Chen, Y.; Feng, X.X.; Li, J.G.; Guo, H.; Miao, P.S.; Jin, R.S.; Tang, C.; Zhao, H.L.; Wang, G.; et al. Uranium occurrence state in the Tarangaole area of the Ordos Basin, China: Implications for enrichment and mineralization. *Ore Geol. Rev.* **2019**, *115*, 103034. [[CrossRef](#)]
6. Chen, Y.; Luo, N.; Chen, L.L.; Miao, P.S.; Li, J.G.; Zhao, H.L.; Li, J.M. Geochemical characteristics of basalts in the northeastern Ordos Basin. *North China Geol.* **2022**, *45*, 1–20.

7. Zhao, H.L.; Chen, L.L.; Feng, X.X.; Li, J.G.; Chen, Y.; Wang, G. Features of Clay Minerals in the Middle Jurassic Zhiluo Formation Sandstones of the Nalinggou Area in the Ordos Basin and a Preliminary Comparison with Adjacent Areas. *Geol. J. China Univ.* **2018**, *24*, 627–636.
8. Zhang, L.; Wu, B.L.; Liu, C.Y.; Lei, K.Y.; Hou, H.Q.; Li, S.; Cun, X.N.; Wang, J.Q. Provenance Analysis of the Zhiluo Formation in the Sandstone-hosted Uranium Deposits of the northern Ordos Basin and Implications for Uranium mineralization. *Acta Geol. Sin.* **2016**, *90*, 3441–3453. (In Chinese with English abstract)
9. Lei, K.Y.; Liu, C.Y.; Zhang, L.; Wu, B.L.; Wang, J.Q.; Cun, X.N.; Sun, L. Detrital Zircon U—Pb Dating of Middle-Late Mesozoic Strata in the Northern Ordos Basin: Implications for Tracing Sediment Sources. *Acta Geol. Sin* **2017**, *91*, 1522–1541.
10. Jiao, Y.Q.; Chen, A.P.; Wang, M.F.; Wu, L.Q.; Yuan, H.T.; Zhang, C.Z.; Xu, Z.C. Genetic analysis of the bottom sandstone of Zhiluo Formation, Northeastern Ordos Basin: Predictive base of spatial orientation of sandstone-type uranium deposit. *Acta Sedimentol. Sin.* **2005**, *3*, 371–379. (In Chinese with English abstract)
11. Yue, L.; Jiao, Y.; Wu, L.; Rong, H.; Tao, Z. In situ characterization of pyrite from multiple microenvironments in middle Jurassic strata, northeastern Ordos Basin, China: Evaluation of synsedimentary/diagenetic fluid evolution. *Sediment. Geol.* **2023**, *452*, 106412. [CrossRef]
12. Jiao, Y.Q.; Wu, L.Q.; Rong, H.; Peng, Y.B.; Miao, A.S.; Wang, X.M. The Relationship between Jurassic coal measures and sandstone-type uranium deposits in the northeastern Ordos Basin, China. *Acta Geol. Sin. (Engl. Ed.)* **2016**, *90*, 2117–2132. [CrossRef]
13. Li, H.K.; Geng, J.Z.; Hao, S.; Zhang, Y.Q.; Li, H.M. Zircon U-Pb dating technique using LA-MC-ICP-MS. *Bull. Mineral. Petrol. Geochem.* **2009**, *28*, 77. (In Chinese)
14. Geng, J.Z.; Li, H.K.; Zhang, J.; Zhou, H.Y.; Li, H.M. Zircon Hf Isotope Analysis by Means of LA-MC-ICP-MS. *Geol. Bull. China* **2011**, *30*, 1508–1513. (In Chinese with English abstract)
15. Liu, Y.S.; Gao, S.; Hu, Z.C.; Gao, C.G.; Zong, K.Q.; Wang, D.B. Continental and oceanic crust recycling-induced melt-peridotite interactions in the Trans-North China Orogen: U-Pb dating, Hf isotopes and trace elements in zircons from mantle xenoliths. *J. Petrol.* **2010**, *51*, 537–571. [CrossRef]
16. Ludwig, K.R. *ISOPLOT/EX 3.0: A Geochronological Toolkit for Microsoft Excel*; Berkeley Geochronology Centre Special Publication: Berkeley, CA, USA, 2003.
17. Rudnick, R.L.; Gao, S. Composition of the Continental Crust. In *The Crust*; Rudnick, R.L., Ed.; Elsevier-Pergamon: Oxford, UK, 2003; pp. 1–64.
18. Taylor, S.R.; McLennan, S.M. *The Continental Crust: Its Composition and Evolution*; Blackwell Scientific Publication: Oxford, UK, 1985.
19. McDonough, W.F.; Sun, S.S. The composition of the Earth. *Chem. Geol.* **1995**, *120*, 223–253. [CrossRef]
20. Sun, S.S.; McDonough, W.F. Chemical and isotopic systematics of oceanic basalts: Implications for mantle composition and processes. *Geol. Soc. Lond. Spec. Publ.* **1989**, *42*, 313–345. [CrossRef]
21. Wu, Y.B.; Zheng, Y.F. Mineralogy of Zircon genesis and its constraints on U-Pb age interpretation. *Chin. Sci. Bull.* **2004**, *49*, 1589–1604. (In Chinese with English abstract) [CrossRef]
22. Sircombe, K.N. Tracing provenance through the isotope ages of littoral and sedimentary detrital zircon, eastern Australia. *Sediment. Geol.* **1999**, *124*, 47–67. [CrossRef]
23. Vermeesch, P. On the visualisation of detrital age distributions. *Chem. Geol.* **2012**, *312*, 190–194. [CrossRef]
24. Pearce, T.H.; Gorman, B.E.; Birkett, T.C. The relationship between major element chemistry and tectonic environment of basic and intermediate volcanic rocks. *Earth Planet. Sci. Lett.* **1977**, *36*, 121–132.
25. Wang, M.; Luo, J.L.; Li, M.; Bai, X.; Cheng, C.; Yan, L. Provenance and Tectonic Setting of Sandstone-Type Uranium Deposit in Dongsheng Area, Ordos Basin: Evidence from U-Pb Age and Hf Isotopes of Detrital Zircons. *Acta Petrol. Sin.* **2013**, *29*, 2746–2758. (In Chinese with English abstract)
26. Liu, P.H.; Liu, F.L.; Cai, J.; Liu, J.H.; Shi, J.R.; Wang, F. Geochronological and geochemical study of the lijiazi mafic granulites from the daqingshan-wulashan metamorphic complex, the central khondalite belt in the north china craton. *Acta Petrol. Sin.* **2013**, *29*, 462–484. (In Chinese with English abstract)
27. Cai, J.; Liu, F.L.; Liu, P.H.; Wang, F.; Shi, J.R. Geochronology of the Paleoproterozoic khondalite rocks from the Wulashan-Daqingshan area, the Khondalite Belt. *Acta Petrol. Sin.* **2015**, *31*, 3081–3106. (In Chinese with English abstract)
28. Li, G.Y.; Li, Z.D.; Wang, J.Y.; Wen, S.B. Formation Age, Geochemical Signatures and Geological Significance of the Gaoyaohai BIF-Type Iron Deposit in the Guyang Greenstone Belt, Inner Mongolia. *J. Jilin Univ. (Earth Sci. Ed.)* **2019**, *49*, 1317–1326. (In Chinese with English abstract)
29. Li, G.Y.; Qiu, L.; Li, Z.D.; Gao, L.; Fu, C.; Wang, J.Y.; Zhang, Q.; Tu, J.R.; Ge, T.F. Closure of the Eastern Paleo-Asian Ocean: Constraints from the Age and Geochemistry of Early Permian Zhaojinggou Pluton in Inner Mongolia (North China). *Miner.* **2022**, *12*, 738. [CrossRef]
30. Wang, L.; Wang, G.H.; Lei, S.B.; Chang, C.J.; Hou, W.R.; Jia, L.Q.; Zhao, G.M.; Chen, H.J. Petrogenesis of Dahuabei Pluton from Wulashan, Inner Mongolia: Constraints from Geochemistry, Zircon U-Pb Dating and Sr-Nd-Hf Isotopes. *Acta Petrol. Sin.* **2015**, *31*, 1977–1994. (In Chinese with English abstract)
31. Liu, Y.F.; Nie, F.J.; Jiang, S.H.; Xi, Z.; Zhang, Z.G.; Xiao, W.; Zhang, K.; Liu, Y. Ore-Forming Granites from Chaganhua Molybdenum Deposit, Central Inner Mongolia, China: Geochemistry, Geochronology and Petrogenesis. *Acta Petrol. Sin.* **2012**, *28*, 409–420. (In Chinese with English abstract)

32. Jiao, Y.Q.; Wu, L.Q.; Peng, Y.B.; Rong, H.; Ji, D.M.; Miao, A.S.; Li, H.L. Sedimentary tectonic setting of the deposition-type uranium deposits forming in the Paleo-Asian tectonic domain, North China. *Earth Sci. Front.* **2015**, *22*, 189–205. (In Chinese with English abstract)
33. Jiao, Y.Q.; Wu, L.Q.; Rong, H. Model of inner and outer reductive media within uranium reservoir sandstone of sandstone-type uranium deposits and its ore-controlling mechanism: Case studies in Daying and Qianjiadian Uranium Deposits. *Earth Sci.* **2018**, *2*, 459–474. (In Chinese with English abstract)

Disclaimer/Publisher's Note: The statements, opinions and data contained in all publications are solely those of the individual author(s) and contributor(s) and not of MDPI and/or the editor(s). MDPI and/or the editor(s) disclaim responsibility for any injury to people or property resulting from any ideas, methods, instructions or products referred to in the content.